Assessing Longitudinal Treatment Efficacies and Alterations in Molecular Markers Associated with Glutamatergic Signaling and Immune Checkpoint Inhibitors in a Spontaneous Melanoma Mouse Model

Kevinn Eddy[1,2], Kajal Gupta[3], Mohamad Naser Eddin[1], Christina Marinaro[1], Sanjana Putta[1], John Michael Sauer Jr[1], Anna Chaly[4], Katie B. Freeman[4], Jeffrey C. Pelletier[4], Anna Fateeva[1,2], Philip Furmanski[1,5,6], Ann W. Silk[7,8], Allen B. Reitz[4], Andrew Zloza[9] and Suzie Chen[1,2,5,6]

Previous work done by our laboratory described the use of an immunocompetent spontaneous melanoma-prone mouse model, TGS (TG-3/SKH-1), to evaluate treatment outcomes using inhibitors of glutamatergic signaling and immune checkpoint for 18 weeks. We showed a significant therapeutic efficacy with a notable sex-biased response in male mice. In this follow-up 18-week study, the dose of the glutamatergic signaling inhibitor was increased (from 1.7 mg/kg to 25 mg/kg), which resulted in improved responses in female mice but not male mice. The greatest reduction in tumor progression was observed in male mice treated with single-agent troriluzole and anti–PD-1. Furthermore, a randomly selected group of mice was removed from treatment after 18 weeks and maintained for up to an additional 48 weeks demonstrating the utility of the TGS mouse model to perform a ≥1-year preclinical therapeutic study in a physiologically relevant tumor–host environment. Digital spatial imaging analyses were performed in tumors and tumor microenvironments across treatment modalities using antibody panels for immune cell types and immune cell activation. The results suggest that immune cell populations and cytotoxic activities of T cells play critical roles in treatment responses in these mice. Examination of a group of molecular protein markers based on the proposed mechanisms of action of inhibitors of glutamatergic signaling and immune checkpoint showed that alterations in expression levels of xCT, γ-H2AX, EAAT2, PD-L1, and PD-1 are likely associated with the loss of treatment responses. These results suggest the importance of tracking changes in molecular markers associated with the mechanism of action of therapeutics over the course of a longitudinal preclinical therapeutic study in spatial and temporal manners.

Keywords: Cancer biology, Drug development, Melanoma, Methods/tools/techniques, Mouse models

JID Innovations (2024);**4:**100262 doi:10.1016/j.xjidi.2024.100262

INTRODUCTION

Melanoma is a lethal skin cancer owing to its propensity to metastasize to distant sites by lymphatic and hematogenous spread. The American Cancer Society estimates that in 2024, about 100,000 new cases of invasive melanoma will be diagnosed, and approximately 8000 patients will die from this disease (Siegel et al., 2024). These grave statistics underscore the importance of developing rationale and safe drug combinations for the assessment of potential therapeutic treatments in a model system that accurately captures human melanoma development and progression as well as improves survival in patients with metastatic melanoma.

Previously, in a long-term therapeutic study using troriluzole, an inhibitor of glutamatergic signaling and anti–PD-1, an immune checkpoint inhibitor in a spontaneous melanoma-prone mouse model, TGS (TG-3/SKH-1), a model system reported to have a physiologically relevant and immunocompetent tumor–host environment, was reported (Eddy et al, 2023). Melanoma in these mice is driven by the ectopic expression of a neuronal receptor, mGluR1 (protein and *Grm1* [mouse gene]). TGS mice harboring 2 copies of the

[1]*Susan Lehman Cullman Laboratory for Cancer Research, Ernest Mario School of Pharmacy, Rutgers University, Piscataway, New Jersey, USA;* [2]*Graduate Program in Cellular & Molecular Pharmacology, School of Graduate Studies, Rutgers University, Piscataway, New Jersey, USA;* [3]*Division of Surgical Oncology, Department of Surgery, Rush University Medical Center, Chicago, Illinois, USA;* [4]*Fox Chase Therapeutics Discovery, Doylestown, Pennsylvania, USA;* [5]*Rutgers Cancer Institute of New Jersey, New Brunswick, New Jersey, USA;* [6]*Environmental & Occupational Health Sciences Institute, Rutgers University, Piscataway, New Jersey, USA;* [7]*Dana-Farber Cancer Institute, Harvard Medical School, Boston, Massachusetts, USA;* [8]*Department of Medicine, Harvard Medical School, Boston, Massachusetts, USA; and* [9]*Division of Hematology, Oncology, and Cell Therapy, Department of Internal Medicine, Rush University Medical Center, Chicago, Illinois, USA*

Correspondence: Suzie Chen, Susan Lehman Cullman Laboratory for Cancer Research, Rutgers University, 164 Frelinghuysen Road, Piscataway, New Jersey 08854, USA. E-mail: suziec@pharmacy.rutgers.edu

Abbreviations: GLS, glutaminase; IVIS, In Vivo Imaging System; MOA, mechanism of action

Received 3 August 2023; revised 22 December 2023; accepted 8 January 2024; accepted manuscript published online XXX; corrected proof published online XXX

Cite this article as: JID Innovations 2024;4:100262

disrupted *Grm1* gene have onset of melanoma within 1.5−2 months and succumb to heavy tumor burden by 4−5 months (homozygous mice), whereas TGS mice with 1 copy of the disrupted *Grm1* allele show onset of melanoma within 4−5 months and succumb to melanoma by 10−12 months (heterozygous mice) (Eddy et al, 2023). The melanoma in heterozygous or homozygous TGS mice is histologically indistinguishable. Metastases are detected in both genotypes and can be found in the lymph nodes, lung, liver, muscle, skull, spleen, and brain (Zhu et al, 1998). It was observed that the aberrant expression of mGluR1 is independent of the sequence variants of *Braf* and *Nras* in the parental TG-3 mice and human patients with melanoma; however, the sequence variants of *Braf* and *Nras* in TGS mice used in these studies were not specifically examined because the onset and progression of pigmented tumors in TGS have not deviated from previous studies (Chen et al., 2018). Tumor development, progression, and immune dysfunctions in these mice resemble those observed in patients with melanoma (Alb et al, 2012; Eddy and Chen, 2021, 2020; Mairhofer et al, 2015; Prokopi et al, 2021; Zhu et al, 2000). In the earlier study, the functional inhibition of mGluR1 by troriluzole and anti−PD-1 yielded antitumor responses but also showed a sex-biased response in male mice (Eddy et al, 2023). A report on a glioblastoma allograft study showed greater efficacy and higher tolerability of troriluzole at 25 mg/kg (Medikonda et al, 2021). These reported results prompted us to initiate a second study with this high dose of troriluzole to assess whether higher treatment responses may be achieved and/or whether the observed sex-biased responses could be eliminated.

In this study, we reported on the treatment responses in TGS mice with the increased troriluzole dose with or without anti−PD-1 as well as detailed evaluations of the immune cell populations and activated T cells and examination of several selected relevant molecular markers associated with the mechanisms of action (MOAs) of troriluzole, a prodrug of riluzole, and anti−PD-1 over the course of the 18-week study.

RESULTS

In vivo graft assessment of combining troriluzole and anti−PD-1

The dose of 1.7 mg/kg troriluzole used in the previous study was based on results from a xenograft study with human melanoma C8161 cells, where it was found that troriluzole at 1.7 mg/kg reduced implanted tumor cell growth by 84% after 21 days (Chen et al, unpublished data). Recently, Medikonda et al (2021) described the use of troriluzole and anti−PD-1 in reducing orthotopically implanted glioblastoma cell growth in C57BL/6 mice with a higher dose of troriluzole without obvious toxicity. On the basis of these data, we performed a preliminary high-dose allograft study with a mGluR1-expressing mouse melanoma cell line, MASS20, and troriluzole at 25 mg/kg in syngeneic C57BL/6 mice (Shin et al, 2008; Zhu et al, 1999). Once the allografted tumors were palpable, we began the study using the prodrug of riluzole, troriluzole, at 25 mg/kg. Once the vehicle-treated group, DMSO + rat IgG, reached the maximum permitted tumor volume (1200 mm^3) as per Rutgers University Institutional Animal Care and Use Committee protocol, the study was terminated for the measurements of tumor volumes. However, mice in the treatment groups that did not reach the maximum permitted tumor volumes were continued in the study until day 29, when the majority of the mice reached the maximum permitted tumor volumes, and mice were killed. We confirmed the earlier study by Medikonda et al (2021) that troriluzole given at 25 mg/kg was tolerable with no obvious toxicity; furthermore, when combined with anti−PD-1, a reduction by 60 or 70% in allografted tumors was observed (Figure 1a). H&E staining on excised liver samples revealed that at 25 mg/kg of troriluzole as a single agent or in combination with anti−PD-1 showed no apparent toxicity after 20−30 days of treatment, and no differences in liver weights were observed at time of killing (Figure 1b and c). Liver specimens used in the H&E staining for the vehicle group (DMSO + rat IgG) were from mice terminated at 14 days owing to large tumor volumes, but for the troriluzole or combination of troriluzole and anti−PD-1, the liver samples were taken from mice in the allograft study at 29 days. After it was established that there was no short-term liver toxicity in immunocompetent C57BL/6 mice treated with the higher dose of troriluzole, we initiated the long-term (18 weeks) study using TGS mice with 25 mg/kg troriluzole with or without anti−PD-1.

Reduced tumor progression in mice treated with single-agent troriluzole and anti−PD-1

TGS mice are immunocompetent hairless spontaneous metastatic melanoma-prone mice that were developed from crosses between the TG-3 and SKH-1 to allow tumor progression to be monitored easily without the inconvenience of fur (Eddy et al, 2023). TG-3 and TGS mice have similar onset and progression of melanoma.

Heterozygous male and female TGS mice aged 7−9 weeks were used for the study. Mice were randomly divided into 4 treatment arms: DMSO (vehicle control for troriluzole) + rat IgG (isotype control for anti−PD-1), troriluzole monotherapy, anti−PD-1 monotherapy, and troriluzole + anti−PD-1 (Figure 2a). At the initiation of the study (0 weeks), all mice were imaged using the small animal imaging system (In Vivo Imaging System [IVIS]), body weights were measured, and blood was taken. These assays were repeated every 6 weeks. Four male and female mice in each treatment group were randomly assigned to be killed at 0, 6, 12, and 18 weeks; livers and tumors were harvested from these mice; liver weights were taken; and tumor samples were used later to assess for molecular changes. The mice that were killed at 0, 6, 12, and 18 weeks were excluded from subsequent analyses of changes in tumor growth and glutamate analyses. Only mice that were in the study for the entire 18 weeks were included in these analyses because we could track tumor growth and glutamate changes without killing mice. At the end of the 18-week treatment study, a randomly selected subset of male and female mice across treatment arms had their treatments ceased and put on the survival study. The maximum period for the survival study was 48 weeks after treatment cessation (Figure 2a).

In the published low-dose troriluzole (1.7 mg/kg) study, male mice responded to all treatment modalities, with the

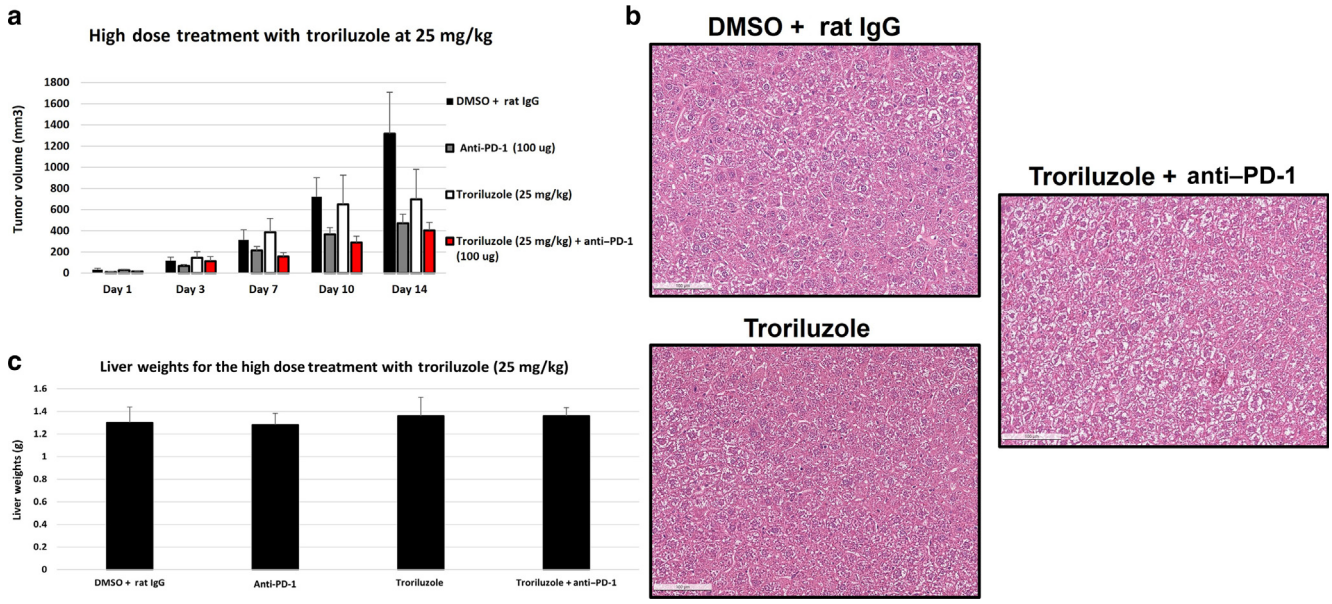

Figure 1. Allograft melanoma model. (**a**) Five C57BL/6 male mice were used for each treatment group. One hundred thousand MASS20 cells were inoculated into both flanks of C57BL/6 mice. When the tumor volumes reached 60–70 mm^3, the tumor-bearing mice were randomly divided into DMSO + rat IgG, anti–PD-1 (100 μg/mouse/injection), troriluzole (25 mg/kg), and troriluzole + anti–PD-1 (same dose as single-agent treatments) groups. Treatments were terminated once the tumor burden reached Rutgers University IACUC tumor burden limits (approximately 1200 mm^3) in any group. In **a**, the tumor volume data are shown until day 14 when DMSO + rat IgG treatment arm reached the tumor burden limits. Data are presented as average tumor volume ± SEM. (**b**) Representative images of liver H&E staining (bar = 100 μM) of DMSO + rat IgG (n = 2 males), troriluzole (n = 3 males), and troriluzole + anti–PD-1 (n = 3 males). (**c**) Average liver weights ± SEM. Liver samples were taken from all 5 C57BL/6 mice used in the allograft study at the termination of the study. The average liver weights were derived from all mice in the study. The histology of the excised liver samples was performed as described. Livers were harvested from all treatment groups at necropsy and immediately placed in 10% neutral buffered formalin (catalog number HT501128-4L, Sigma-Aldrich). After 72 hours, formalin was replaced with 70% ethanol (catalog number ES753, Azer Scientific, Morgantown, PA). The samples were stored until they were processed to paraffin blocks and H&E stained by HistoWiz (Brooklyn, NY). Representative images of liver H&E were taken from the HistoWiz website (https://home.histowiz.com/), and the liver H&E slides were further evaluated for liver toxicity by the HistoWiz pathologist. IACUC, Institutional Animal Care and Use Committee.

most reduction in tumor progression from baseline in the monotherapy of troriluzole (12%) or anti–PD-1 (0%) treatment arm compared with that in vehicle treatment (65%) (Eddy et al, 2023). In this study, at the higher dose of troriluzole (25 mg/kg), the greatest reduction in tumor progression from baseline was observed in male mice treated with single-agent troriluzole (69%) or anti–PD-1 (46%) than in those treated with vehicle (91%) (Figure 2b). In this study, the female mice showed the greatest percentage change in tumor progression from baseline belonging to the anti–PD-1 (94%) or combination or troriluzole and anti–PD-1 group (78%) than in the vehicle-treated group (64%). In contrast, female mice treated with the single-agent troriluzole showed the lowest percentage change in tumor progression from baseline (50%) than those treated with vehicle (64%), suggesting that at the higher dose of troriluzole, female mice may benefit more (Figure 2b). An unexpected result was the outcome in the anti–PD-1–treated male mice. The dose of anti–PD-1, the company where we purchased anti–PD-1, and the treatment methods were the same as previously reported in the lower-dose troriluzole study (Eddy et al, 2023). To note, between the lower-dose troriluzole study and the higher-dose troriluzole study, there was an 18–24-month gap, and this may account for this discrepancy. The lot/batch numbers of the purchased anti–PD-1 (BioXCell [clone: RMP1-14; catalog number BE0146]) were different, and TGS mice used for the studies were bred 18–24 months apart in house; however, the husbandry at our institution remains unchanged for the past several years. No alterations in the body and liver weights and no histopathological liver toxicity were detected by H&E analysis from the mice in the 18-week longitudinal studies (Figure 3).

Liquid chromatography–tandem mass spectrometry was used to determine the circulating concentrations of glutamate in the blood plasma of treated mice. Previous work from our group demonstrated higher levels of glutamate in conditioned media in in vitro cultured mGluR1-positive melanoma cells, and the inclusion of riluzole resulted in reduced glutamate levels (Namkoong et al, 2007; Shin et al, 2008). However, in the current in vivo study, no difference was observed in systemic circulating glutamate levels, confirming the observations in the lower-dose troriluzole study (Figure 4) (Eddy et al, 2023).

Loss of response over the course of 18 weeks in the troriluzole and/or anti–PD-1 treatment arms

All mice in the treatment groups were classified into responders or nonresponders on the basis of a modified RECIST (Response Evaluation Criteria in Solid Tumors) criteria that calculated the percentage change in tumor burden from baseline (0 weeks, treatment initiation) to 6, 12, and 18 weeks on treatment (Eddy et al, 2023; Eisenhauer et al, 2009). The RECIST criteria are used by oncologists to objectively ascertain whether a treatment regimen is effective in shrinking a patient's tumor(s). Quantitatively, these criteria define progressive disease as at least a 20% increase and partial response as at least a 30%

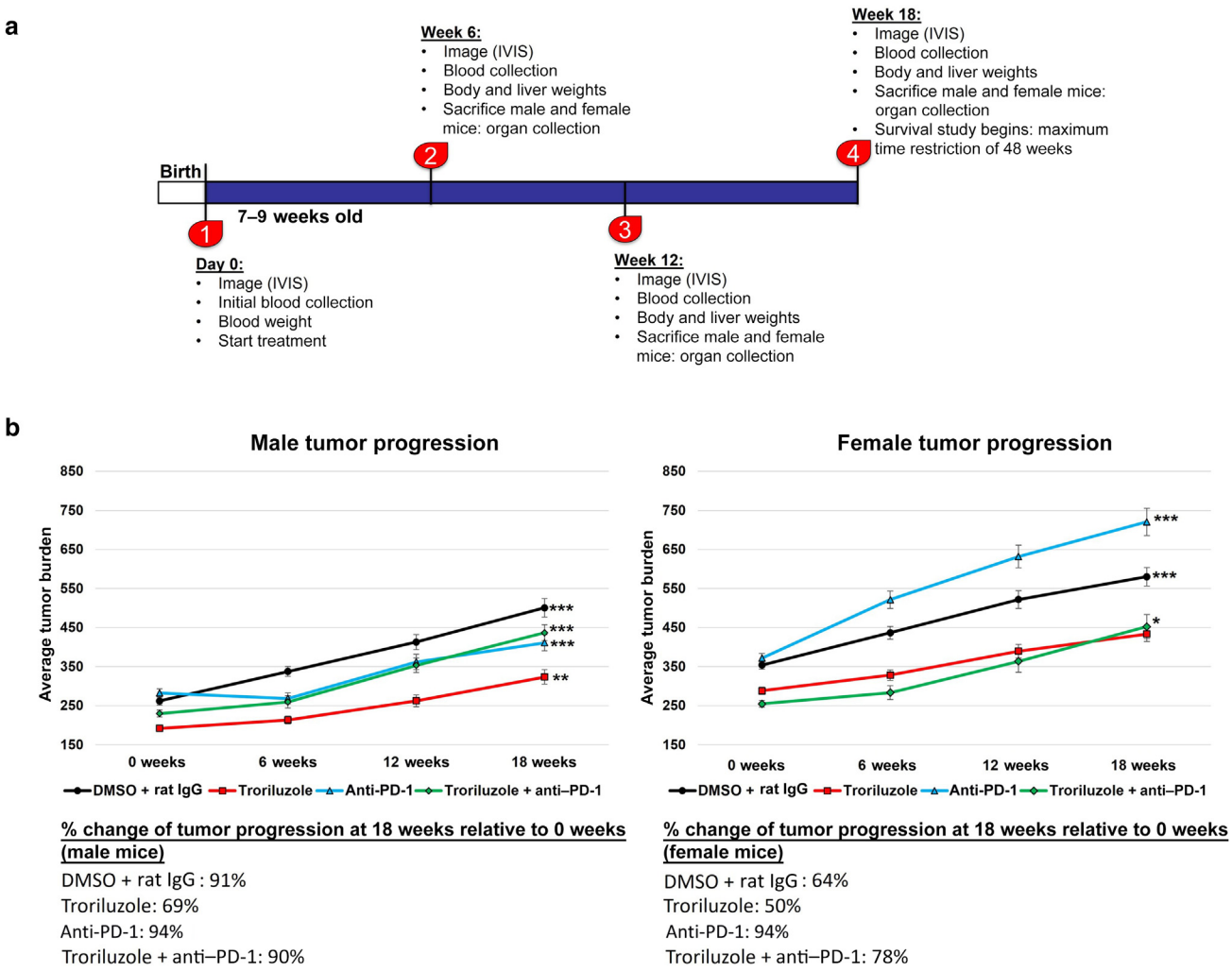

Figure 2. Treatments with inhibitors of glutamatergic signaling (troriluzole) or immune checkpoint (anti−PD-1) reduced the percentage change of tumor progression at 18 weeks relative to that at 0 weeks in males. (**a**) Experimental design of the study. (**b**) Data shown included only mice that were on treatment for the entire 18 weeks of study: vehicle (DMSO + rat IgG, n = 8 males, n = 8 females), troriluzole (n = 8 males, n = 8 females), anti−PD-1 (n = 12 males, n = 10 females), and troriluzole + anti−PD-1 (n = 8 males, n = 8 females). Tumor burden (units: pixel^2) was defined as the size and pigmentation of the tumors. Percentage change in tumor progression at 18 weeks was calculated as a percentage change between 0 and 18 weeks for each respective treatment arm. Statistical significance was determined using 2-way ANOVA tests with Bonferroni posthoc comparisons for each sex where the exposure variables were treatments and time points (0, 6, 12, and 18 weeks), and the outcome variable was tumor burden. Comparisons between 0 and 18 weeks male mice for vehicle (DMSO + Rat IgG) (P = 1.11E-8), troriluzole (P = .003), anti−PD-1 (P = .0002), and troriluzole + anti−PD-1 (P = 7.20E-7) was performed. Comparisons between 0 and 18 weeks female mice for vehicle (P = .001), anti−PD-1 (P = 5.47E-9), and troriluzole + anti−PD-1 (P = .007). *P < .05, **P < .005, and ***P < .001. IVIS, In Vivo Imaging System.

decrease, whereas stable disease is defined as disease with neither sufficient shrinkage to qualify for partial response nor sufficient increase to qualify for progressive disease (Eisenhauer et al, 2009). The criterion we used to define nonresponders is ≥20% change from baseline for mice with progressive disease, whereas partial response and stable disease were considered responders (≤19.9% change from baseline) (Eddy et al, 2023). This criterion was used for both treated and control arms, where the distribution of tumor growth in the control arm represented the natural variation of the arm.

Heterogenous responses to troriluzole and/or anti−PD-1 were observed in both sexes, and reduced responses were observed across all treatment arms over time, suggesting a loss of response to the treatment regimens (Figure 5). During the first evaluation at 6 weeks, at least 50% of male mice were classified as having partial response or stable disease (Figure 5a). As the treatments continued, most of the male mice except for 13−25% were grouped in the progressive disease category (Figure 5a). In contrast, most female mice exhibited little benefit, and the response rates remained unchanged until the end of the study (Figure 5b). The only exception was in the combination arm where over 50% of the female mice at 6 weeks showed stable disease or partial response, and this gradually decreased to only 25% by the end of the study at 18 weeks (Figure 5b). No complete response was observed in this study.

Survival outcomes in male and female TGS mice treated with troriluzole and/or anti−PD-1 48 weeks after treatment cessation

This longitudinal study was terminated after 18 weeks of treatment, and a subset of male and female mice was

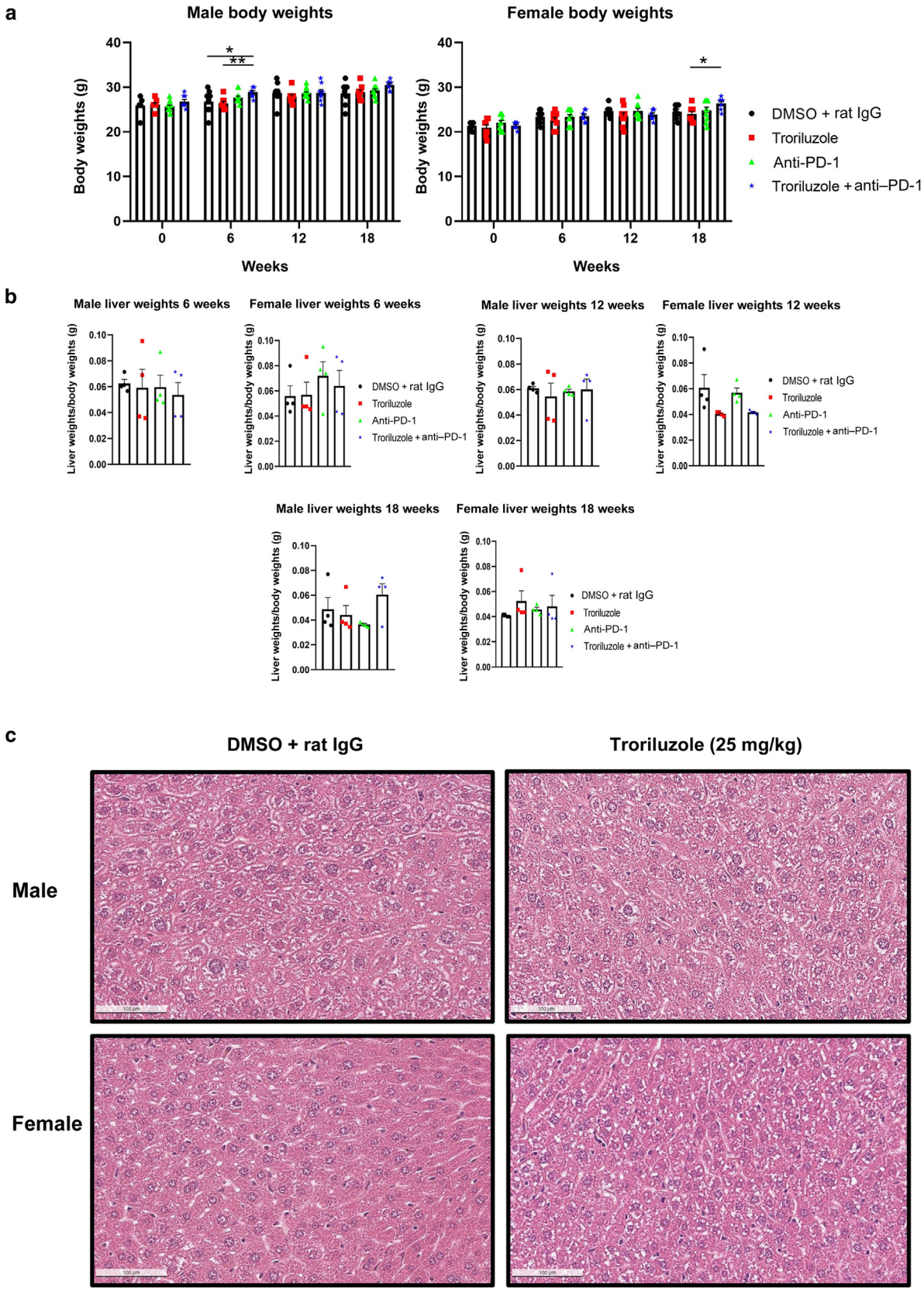

Figure 3. Evaluation of treatment toxicity. (**a**) Average body weight ± SEM. Treatment arms and sample sizes are the same as in Figure 2. (**b**) Average liver weights normalized to their respective body weights ± SEM. Four male and 4 female mice were randomly killed at 0, 6, 12, and 18 weeks, and these mice were not included in the analysis for tumor growth (Figure 2) and glutamate analysis (Figure 4). Livers were weighed from mice from all treatment groups at necropsy at 0, 6, 12, and 18 weeks. (**c**) Representative images of liver H&E staining (bar = 100 μM). DMSO + rat IgG (n = 3 males, n = 3 females) and troriluzole (n = 3 males, n = 1 females). Statistical significance between treated pairs was conducted for each sex using either a 1-way or 2-way ANOVA test depending on the

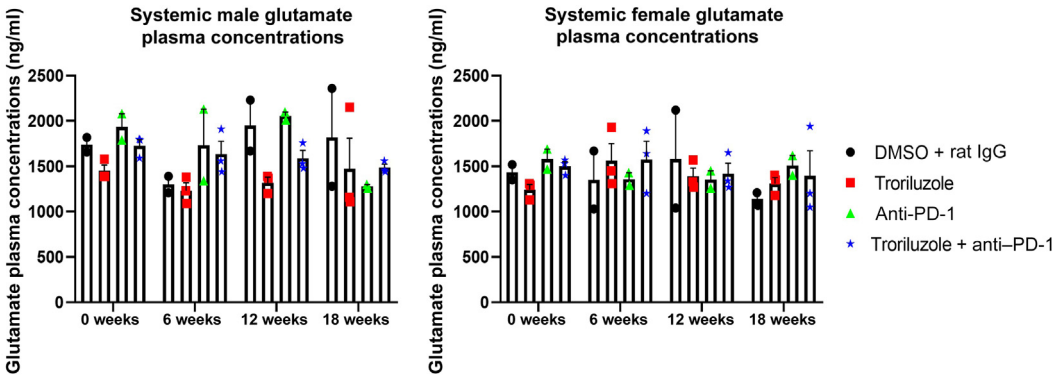

Figure 4. Systemically circulating glutamate levels over the course of treatments in male and female mice. Pharmacokinetic bioanalyses were conducted by LC-MS/MS on blood plasma collected at 0, 6, 12, and 18 weeks from the same mouse. Blood plasma was collected through retroorbital bleeding at least 20 hours after treatment. Averages values were determined from at least 2−3 different mice and are shown as average glutamate levels ± SEM. Statistical analyses were conducted for each sex using a 2-way ANOVA test with Bonferroni posthoc comparisons to determine statistical significance between treated pairs where the exposure variables were treatments and time points (0, 6, 12, and 18 weeks), whereas the outcome variable was glutamate concentration. LC-MS/MS, liquid chromatography−tandem mass spectrometry.

randomly chosen and had treatment ceased before being placed in the survival study. The survival study was performed for a maximum of 48 weeks (336 days) after treatment cessation or until the mouse reached Rutgers University Institutional Animal Care and Use Committee tumor burden limits: the size and thickness of the lesions on the ears, the eyelid, and the snout were >5 mm, and those in the perianal region were >8 mm.

Overall, the male and female mice in the anti−PD-1 treatment arm showed the highest proportion of mice surviving (50%) than those in the other treatment modalities at the completion of the study (336 days), and they may have lived longer if the study continued, albeit they were a small sample size with at least 4 male and female mice in each group, and no statistical significance was observed (Figure 6). A higher number of mice were in the anti−PD-1 treatment arm and may have skewed survival outcomes (Figure 6). The Gehan−Breslow−Wilcoxon statistical test was the primary test used because of the crossing of the survival curves. This test does not require a consistent hazard ratio but does require that 1 group consistently have a higher risk than the other. If the 2 survival curves cross, then 1 group has a higher risk at early time points, and the other group has a higher risk at later time points, which was not the case in this survival study. This could just be a coincidence of random sampling, and the assumption of proportional hazards could still be valid. A total of 25% of male or female mice in the troriluzole treatment arm survived until the end of the study, and they may have lived longer if the study continued (Figure 6). Regardless of the treatment modality, overall, male mice survived longer than female mice (Figure 6). Interestingly, male mice treated with either single-agent troriluzole or combined with anti−PD-1 succumbed to disease faster than those treated with vehicle controls (Figure 6). The tumor burden for each mouse at the start of the survival study did not correlate with survival outcomes (Table 1).

Evaluation of protein expression in excised tumor samples using a set of molecular markers associated with the MOA of troriluzole, a prodrug of riluzole, and anti−PD-1

Possible changes in protein expression of relevant markers in excised tumor samples from male and female mice killed at 6, 12, and 18 weeks were examined. Mice were randomly selected at each time point and showed tumor phenotypes similar to those of mice that remained in the study.

The expression of the following proteins was evaluated by western immunoblots on the basis of the potential MOA of troriluzole, a prodrug of riluzole, and anti−PD-1: mGluR1, glutaminase (GLS), xCT, γ- H2AX, EAAT2, PD-L1, and PD-1. Tyrosinase, a melanocyte-specific marker, was used for normalization instead of the commonly used housekeeping proteins. Earlier work showed that only mGluR1-positive melanoma cells were sensitive to riluzole (Namkoong et al, 2007; Shah et al, 2019). GLS is an enzyme that converts glutamine to glutamate before entering the tricarboxylic acid cycle and may contribute to the establishment of autocrine/paracrine loops in mGluR1-expressing melanoma cells. xCT is an antiporter that exports 1 molecule of glutamate to the outside of the cells and imports 1 molecule of cystine into the cell (Shah et al, 2019; Shin et al, 2018). Riluzole has been postulated to mediate its inhibition of the export of glutamate through interruption of xCT, thus disrupting the exchange of glutamate and cystine, resulting in less import of cystine and a decrease of cysteine, the reduced form of cystine, to participate in glutathione synthesis (Wall et al, 2014). A reduction in glutathione will contribute to elevated levels of ROS and DNA damage as shown by an increase in γ-H2AX, a marker of DNA damage (Wall et al, 2014). EAAT2, a glutamate transporter for glutamate reuptake, has been shown to be upregulated upon riluzole treatment (Carbone et al, 2012; Shin et al, 2018). PD-L1 and PD-1 are associated with the MOA of anti−PD-1 where they have canonical roles in immune evasion. In addition, the PD-1/PD-L1 axis

variable(s) being tested, and Bonferroni posthoc analysis was used during 2-way ANOVA. The exposure and outcome variables for the 1-way ANOVA were treatment groups and liver weights normalized to body weights, respectively, whereas for the 2-way ANOVA, the exposure and outcome variables were treatments and time points (0, 6, 12, and 18 weeks) and body weights, respectively. *$P < .05$ and **$P < .01$.

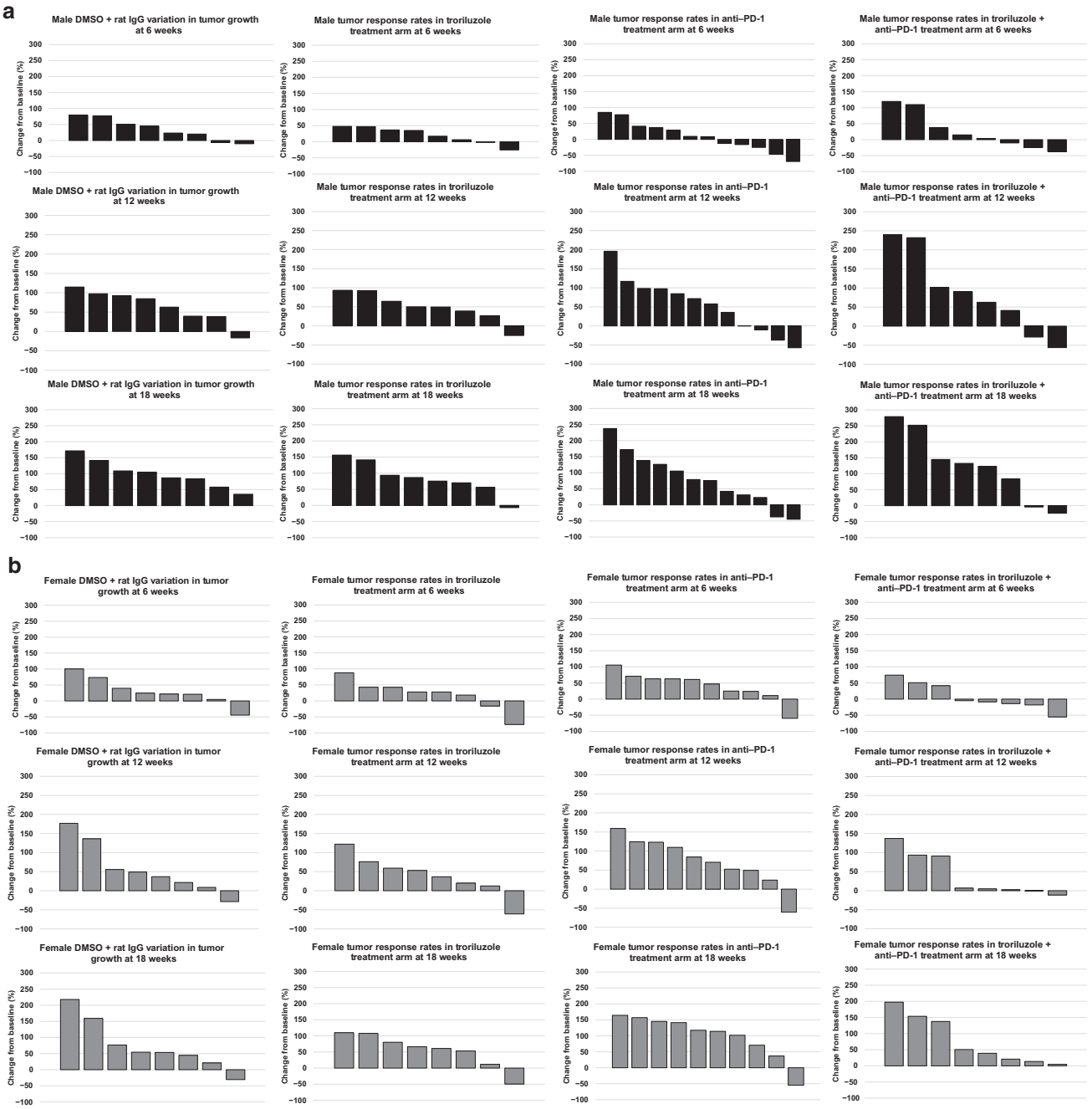

Figure 5. Changes in tumor response over the course of 6, 12, and 18 weeks in male and female mice treated with troriluzole and/or anti−PD-1. All mice were monitored throughout the 18-week study, and tumor responses were calculated using the percentage change from baseline at (0 weeks) to 6, 12, and 18 weeks. Treatment arms: vehicle (DMSO + rat IgG, n = 8 males, n = 8 females), troriluzole (n = 8 males, n = 8 females), anti−PD-1 (n = 12 males, n = 10 females), and troriluzole + anti−PD-1 (n = 8 males, n = 8 females). (**a**) Black bars represent male mice. The top panel represents tumor response rates at 6 weeks, the middle panel represents tumor response rates at 12 weeks, and the bottom panel represents tumor response rates at 18 weeks. (**b**) Gray bars represent female mice. The top panel represents tumor response rates at 6 weeks, the middle panel represents tumor response rates at 12 weeks, and the bottom panel represents tumor response rates at 18 weeks.

within the tumor also has tumor-intrinsic functions, including tumor growth, metastatic signaling, and tumor-suppressive roles (Clark et al, 2016; Kleffel et al, 2015; Wang et al, 2020).

Comparisons of protein expression levels in tumor samples from 6 and 18 weeks showed that mGluR1 and GLS expression remained stable over the course of 18 weeks in male and female mice (Figure 7). xCT expression in male and female mouse tumors was lower at 6 weeks, which was defined as early in the treatment regimen, and increased as response rates decreased with time. Similarly, higher levels of γ-H2AX were noted early but decreased with time in male mice, suggesting that the targeted cells became less sensitive to troriluzole, as illustrated by the lower responses with time. In female tumors, γ-H2AX expression was unchanged. EAAT2 expression increased over time in both male and female mice across treatment arms, suggesting that it may be

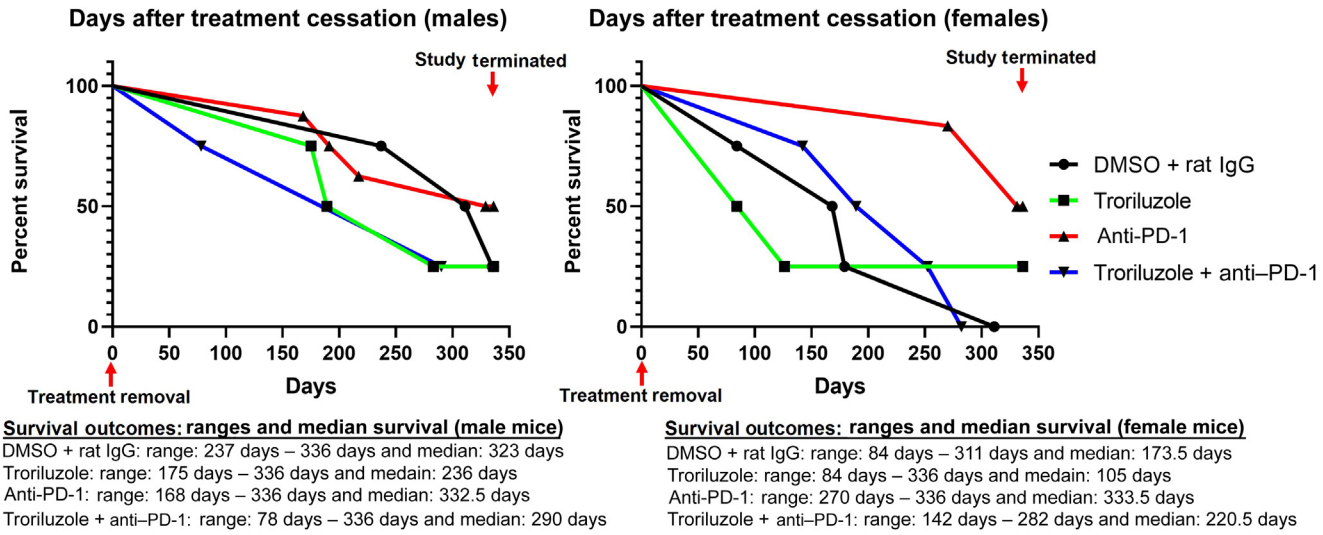

Figure 6. Survival outcomes in male and female mice after treatment cessation. After 18 weeks of treatment, a random subset of male and female TGS mice in each treatment arm was taken off treatment to determine their survival outcomes. Treatment arms: vehicle (DMSO + rat IgG, n = 4 males, n = 4 females), troriluzole (n = 4 males, n = 4 females), anti–PD-1 (n = 8 males, n = 6 females), and troriluzole + anti–PD-1 (n = 4 males, n = 4 females). The Log-rank (Mantel–Cox) and Gehan–Breslow–Wilcoxon statistical tests were used to evaluate the significance of each treatment compared with the vehicle group, DMSO + rat IgG, and also the significance of the monotherapies with the combination therapies. Both statistical tests showed similar outcomes. The Gehan–Breslow–Wilcoxon statistical test was the primary test used because of the crossing of the survival curves. The Bonferroni's adjusted alpha value used was 0.002.

necessary for the mice to maintain the homeostatic balance of glutamate concentrations for the proper functions of the tricarboxylic acid cycle and may also compensate for the lack of alterations in GLS despite the increasing xCT expression (Eddy and Chen, 2021; Shah and Chen, 2020). PD-L1 expression increased over time in male and female mice, particularly in the anti–PD-1 treatment arm, which corresponded with the GeoMx spatial data (Figures 8 and 9). In contrast, PD-1 expression in male and female mice decreased over time (Figure 7). The conflicting differential expression between PD-L1 and PD-1 and the reduction in treatment response support the notion that the PD-L1/PD-1 axis acts as a tumor suppressor (Wang et al, 2020).

Temporal alterations in digital spatial profiles of immune cell populations

GeoMx digital spatial imaging profiles were performed on tissue samples from male and female mice across all treatment arms at 6, 12, and 18 weeks to assess for longitudinal changes in immune cell infiltrates and cytotoxic T cells within the tumors and tumor–stromal interfaces. Mice were randomly selected to be killed at each time point and showed tumor phenotypes similar to those of mice that remained in the study. The GeoMx digital spatial profiler is fundamentally a high-throughput immunohistochemistry assay that provides a means to examine changes in multiple markers within a defined region(s) of a sample simultaneously (Hernandez et al, 2022). Selected antibody panels for immune cell populations and activation markers based on the well-established mechanisms of anti–PD-1 in enhancing antitumor immune response by modulating immune cell infiltration and cytotoxic T cells were used (Eddy and Chen, 2020; Somasundaram et al, 2021; Wang et al, 2021). Immune infiltration of macrophages, $CD8^+$ T cells, $CD4^+$ T cells, and total CD45 immune cell populations as well as cytotoxic T cells in tumors and tumor–stromal interfaces were evaluated in male and female mouse tumor samples isolated from 0, 6, 12, and 18 weeks. Multiple markers were used to validate the immune cell populations observed within and surrounding the tumors (Figures 8 and 9). In general, the markers within each treatment arm correlated well with each other, further validating the observations.

In the tumor–stromal interfaces of male and female mice, loss of total immune cell populations, including macrophages, $CD8^+$ T cells, $CD4^+$ T cells, and cytotoxic T cells, was noted as response frequency decreased with time across all treatment arms (Figure 8). Interestingly, in male but not female mice, loss of activated T cells in the tumor–stromal interfaces correlated with decreasing response rates with time. Within the tumors of male and female mice, loss of macrophages, $CD4^+$ T cells, total immune cell populations, and cytotoxic and activated T cells but not $CD8^+$ T cells was noted as responses decreased with time across all treatment arms (Figure 9). Surprisingly, the combination troriluzole + anti–PD-1 treatment in male and female mice seemed to eliminate the possible benefits of single-agent troriluzole treatment at 18 weeks that led to a reduction of immune cells in the tumor–stromal interfaces and tumors, which correlated with reduced tumor progression as calculated by percentage changes from baseline at 0 weeks to 18 weeks in both sexes (Figures 8 and 9). Representative images of GeoMx scans and region selections are shown in Figure 10.

DISCUSSION

Aberrant mGluR1 expression has been observed in approximately 92% of human melanoma cell lines, with little or no expression detected in human melanocytes, as well as in about 60% of primary and metastatic human melanoma biopsies, with close to 90% detected in metastatic samples

Table 1. Tumor Burden for Mice in the Survival Study

Tumor Burden at the Start of the Survival Study Male Mice

	0 Weeks Tumor Burden	6 Weeks Tumor Burden	12 Weeks Tumor Burden	18 Weeks Tumor Burden	Last Time Point in the Survival Study
DMSO + rat IgG 2240 male	352	333	487	556	687
DMSO + rat IgG 2241 male	382	471	533	703	750
DMSO + rat IgG 2267 male	264	237	220	358	531
DMSO + rat IgG 2268 male	157	227	310	426	481
Troriluzole 2289 male	328	321	416	513	619
Troriluzole 2290 male	170	181	280	329	541
Troriluzole 2292 male	342	255	256	318	503
Troriluzole 2333 male	159	215	239	279	420
Anti–PD-1 2184 male	120	213	355	405	635
Anti–PD-1 2185 male	336	461	620	800	1072
Anti–PD-1 2198 male	92	119	158	250	455
Anti–PD-1 2199 male	426	228	267	266	320
Anti–PD-1 2226 male	372	278	372	488	604
Anti–PD-1 2227 male	343	634	678	613	851
Anti–PD-1 2230 male	190	208	377	390	606
Anti–PD-1 2236 male	188	266	408	425	602
Troriluzole + anti–PD-1 2373 male	192	199	271	353	529
Troriluzole + anti–PD-1 2374 male	172	361	571	652	806
Troriluzole + anti–PD-1 2434 male	424	321	303	406	476
Troriluzole + anti–PD-1 2435 male	341	215	149	260	331

	0 Weeks Tumor Burden	6 Weeks Tumor Burden	12 Weeks Tumor Burden	18 Weeks Tumor Burden	Last Timepoint in the Survival Study
Average DMSO + rat IgG male	288.75	317.00	387.50	510.75	612.25
Average troriluzole male	249.75	243.00	297.75	359.75	520.75
Average anti–PD-1 male	258.38	300.88	404.38	454.63	643.13
Average troriluzole + anti–PD-1 male	282.25	274.00	323.50	417.75	535.50

Tumor Burden at the Start of the Survival Study, Female Mice

	0 Weeks Tumor Burden	6 Weeks Tumor Burden	12 Weeks Tumor Burden	18 Weeks Tumor Burden	Last Timepoint in the Survival Study
DMSO + rat IgG 2262 female	293	587	811	932	995
DMSO + rat IgG 2263 female	436	242	312	302	424
DMSO + rat IgG 2264 female	522	635	812	922	1122
DMSO + rat IgG 2265 female	410	496	561	633	690
Troriluzole 2308 female	356	508	627	740	843
Troriluzole 2310 female	335	88	131	169	164
Troriluzole 2311 female	198	234	223	303	530
Troriluzole 2364 female	252	322	401	454	543
Anti–PD-1 2186 female	356	732	923	941	1000
Anti–PD-1 2187 female	624	916	931	1065	910
Anti–PD-1 2188 female	311	506	573	628	728
Anti–PD-1 2189 female	312	533	696	765	854
Anti–PD-1 2242 female	334	544	700	859	850
Anti–PD-1 2243 female	388	625	870	844	937
Troriluzole + anti–PD-1 2437 female	365	517	706	926	1152
Troriluzole + anti–PD-1 2439 female	298	257	312	414	761

(*continued*)

Table 1. Continued

Tumor Burden at the Start of the Survival Study, Female Mice

	0 Weeks Tumor Burden	6 Weeks Tumor Burden	12 Weeks Tumor Burden	18 Weeks Tumor Burden	Last Timepoint in the Survival Study
Troriluzole + anti–PD-1 2440 female	164	286	389	488	563
Troriluzole + anti–PD-1 2441 female	123	55	109	129	239

	0 Weeks Tumor Burden	6 Weeks Tumor Burden	12 Weeks Tumor Burden	18 Weeks Tumor Burden	Last Time in the Survival Study
Average DMSO + rat IgG female	415.25	490.00	624.00	697.25	807.75
Average troriluzole female	285.25	288.00	345.50	416.50	520.00
Average anti–PD-1 female	387.50	642.67	782.17	850.33	879.83
Average troriluzole + anti–PD-1 female	237.50	278.75	379.00	489.25	678.75

Top, male; bottom, female. Tumor burden (units: pixel^2) was defined as the size and pigmentation of the tumors.

(Eddy and Chen, 2021). The metabotropic glutamate receptor family belongs to the G-protein coupled receptor family and is normally expressed in the CNS where it performs various functions, including memory and learning (Eddy et al, 2022). However, in the last 25 years, many members of the mGluR family have been implicated in various cancer types (Eddy and Chen, 2021; Eddy et al, 2022). It was shown that when mGluR1 is abnormally expressed in mouse melanocytes, one of the consequences is a melanocytic transformation in vitro and spontaneous metastatic melanoma formation in vivo with 100% penetrance (Chen et al, 1996; Eddy and Chen, 2021; Pollock et al, 2003; Shin et al, 2008; Zhu et al, 1998). Furthermore, it has been shown that the oncogenic functions of mGluR1 in our transgenic mice and human melanoma biopsies were independent of *BRAF* and *NRAS* sequence variants (Chen et al., 2018; Eddy et al., 2022). Through genetic and pharmacological approaches, our group and others have shown that sustained expression and functional mGluR1 are required for the maintenance of the transformed phenotypes in vitro and in vivo (Namkoong et al, 2007; Ohtani et al, 2008; Shin et al, 2008; Wangari-Talbot et al, 2012). It has also been demonstrated that elevated levels of glutamate, the natural ligand of mGluR1, are present in conditioned media of mGluR1-expressing melanoma cells to ensure the constitutive activation of the receptor and stimulation of the downstream MAPK and phosphoinositide 3-kinase/protein kinase B pathways involved in cell growth, replicative immortality, apoptosis, angiogenesis, and metastasis (Eddy and Chen, 2021; Marín et al, 2006; Namkoong et al, 2007; Shin et al, 2010, 2008). It was reasoned that limiting the availability of the ligand, glutamate, in the tumor microenvironment of mGluR1-expressing melanoma cells dampens the receptor activity and may be a viable treatment option for patients with metastatic melanoma (Mehnert et al, 2018; Yip et al, 2009).

Several agents that have been used to reduce circulating glutamate were tested, and riluzole was shown to be the most effective compound in reducing the growth of mGluR1-expressing melanoma cells in vitro and tumorigenesis in vivo (Namkoong et al, 2007). Riluzole is a Food and Drug Administration–approved treatment for amyotrophic lateral sclerosis, a debilitating disease characterized by the hyperactivation of glutamate receptors on motor neurons that results in their excitotoxicity. One of the MOAs of riluzole is the inhibition of the release of cellular glutamate, thereby reducing glutamate levels for stimulation of glutamate receptor signaling and neuronal death (Fang et al, 2018). These preclinical findings were used to establish phase 0 and phase II clinical trials in patients with late-stage melanoma. mGuR1 expression was not a selection criterion to participate in the trial; however, all patients enrolled were mGluR1 positive and independent of the sequence variants of *BRAF* or *NRAS*, which are the 2 most frequently detected sequence variants in melanoma (Mehnert et al, 2018; Yip et al, 2009). Comparisons between pairs of pre and posttreatment samples showed a significant decrease in tumor burden assessed by fludeoxyglucose-18-positron emission tomography scans, a reduction in activated MAPK and phosphoinositide 3-kinase/protein kinase B signaling cascades, and stable disease in about 46% of patients treated with riluzole (Mehnert et al, 2018; Yip et al, 2009).

The clinical pharmacology of riluzole is characterized by high levels of patient-to-patient variability owing to the heterogeneous expression of the liver cytochrome P450 isoform CYP1A2 (van Kan et al, 2005). To circumvent this, a prodrug of riluzole, troriluzole, was developed (Eddy et al, 2023). Troriluzole was shown to be safe and tolerable in patients with cancer (Silk et al, 2022). Our rationale for combining troriluzole with anti–PD-1 was based on the clinical data that showed that riluzole could enhance immune cell infiltration in patients with stable disease (Mehnert et al, 2018). In addition, pairs of pre and post-tumor biopsies from a completed phase II trial were examined for γ-H2AX levels, a marker of DNA double-strand breaks. Elevated levels of γ-H2AX were detected only in post-treatment samples from patients with stable disease and not in samples from those with progressive disease (Wall et al, 2014). In addition, it was postulated that riluzole mediates its inhibitory function of exporting glutamate by interfering with the glutamate/cystine antiporter, xCT. This

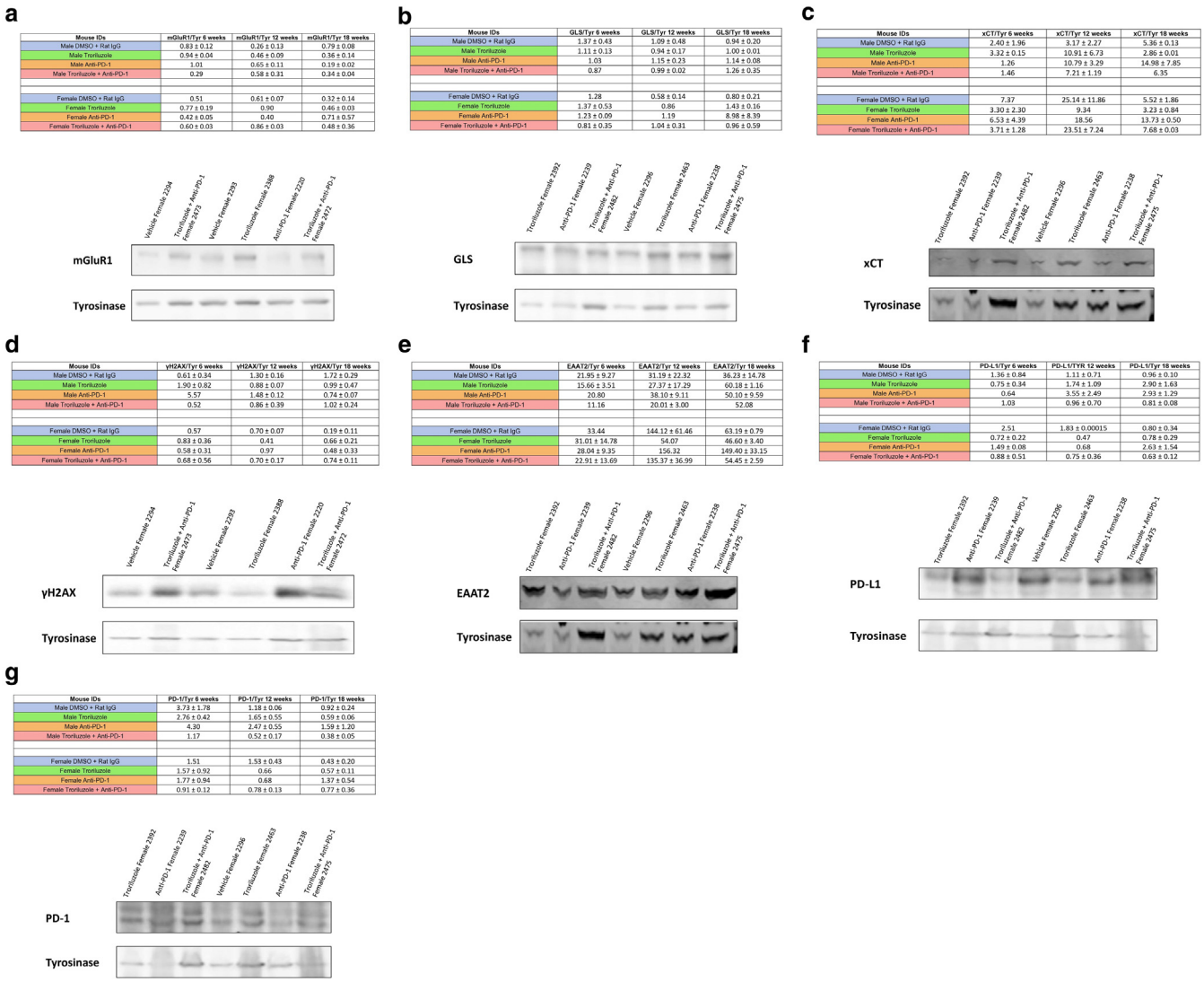

Figure 7. Quantifications and representative western immunoblots for the expression profiles of the molecular markers in melanomas. (**a**) mGluR1, (**b**) GLS, (**c**) xCT, (**d**) γ-H2AX, (**e**) EAAT2, (**f**) PD-L1, and (**g**) PD-1 bands were normalized to their respective tyrosinase bands, and these values were used for subsequent data analyses. The values in the table represent the average intensity of the protein band normalized to their respective tyrosinase band ± SEM. Below the tables are representative western blots associated with their respective proteins, where for mGluR1 and γ-H2AX, the immunoblots represent 12 weeks female mice, and for the GLS, xCT, EAAT2, PD-L1, and PD-1, the immunoblots represent 6 weeks female mice. The threshold used to define change/no change is associated with quantitative changes of 40–50% in protein expression observed between 6 and 18 weeks. At least 2 male and 2 female mice were used except for 6 weeks (male, anti–PD-1 and troriluzole + anti–PD-1; female, DMSO + rat IgG), 12 weeks (female, troriluzole and anti–PD-1), and 18 weeks xCT and EAAT2 (male, troriluzole + anti–PD-1) where only 1 mouse was used. These mice were randomly selected to be killed at 0, 6, 12, and 18 weeks to harvest livers and pigmented tumors. When pigmented tumors were harvested from each mouse, each specimen contained at least 4–6 pieces of independent tumors from that mouse, and western immunoblots were normalized to tyrosinase to consider only melanocytes/melanomas and not other cell types. To note, although we cannot completely exclude the contributions of melanocytes/nonmelanomas in the samples, we ensured during tumor harvest that only pigmented tumors were harvested with little to no adjacent normal skin present. GLS, glutaminase.

hypothesis is based on in silico analysis where the molecular docking sites of riluzole and glutamate are very close to each other in xCT. It is possible that riluzole may partially block the glutamate-binding site on xCT, thus reducing the export of glutamate, leading to less import of cystine and consequently low levels of cysteine available to participate in glutathione synthesis, and thereby increasing ROS and DNA damage (Eddy et al, 2022; Shin et al, 2018). In addition, the preferential DNA repair pathway in riluzole-treated melanoma cells is the error-prone nonhomologous end-joining repair pathway (Cerchio et al, 2020). If not repaired, damaged DNA could contribute to the sequence variant burden of tumor cells and potentially enhance their neoantigen load. This, in addition to reducing extracellular glutamate to stimulate mGluR1, formed the basis of the working hypothesis that riluzole/troriluzole contributes to

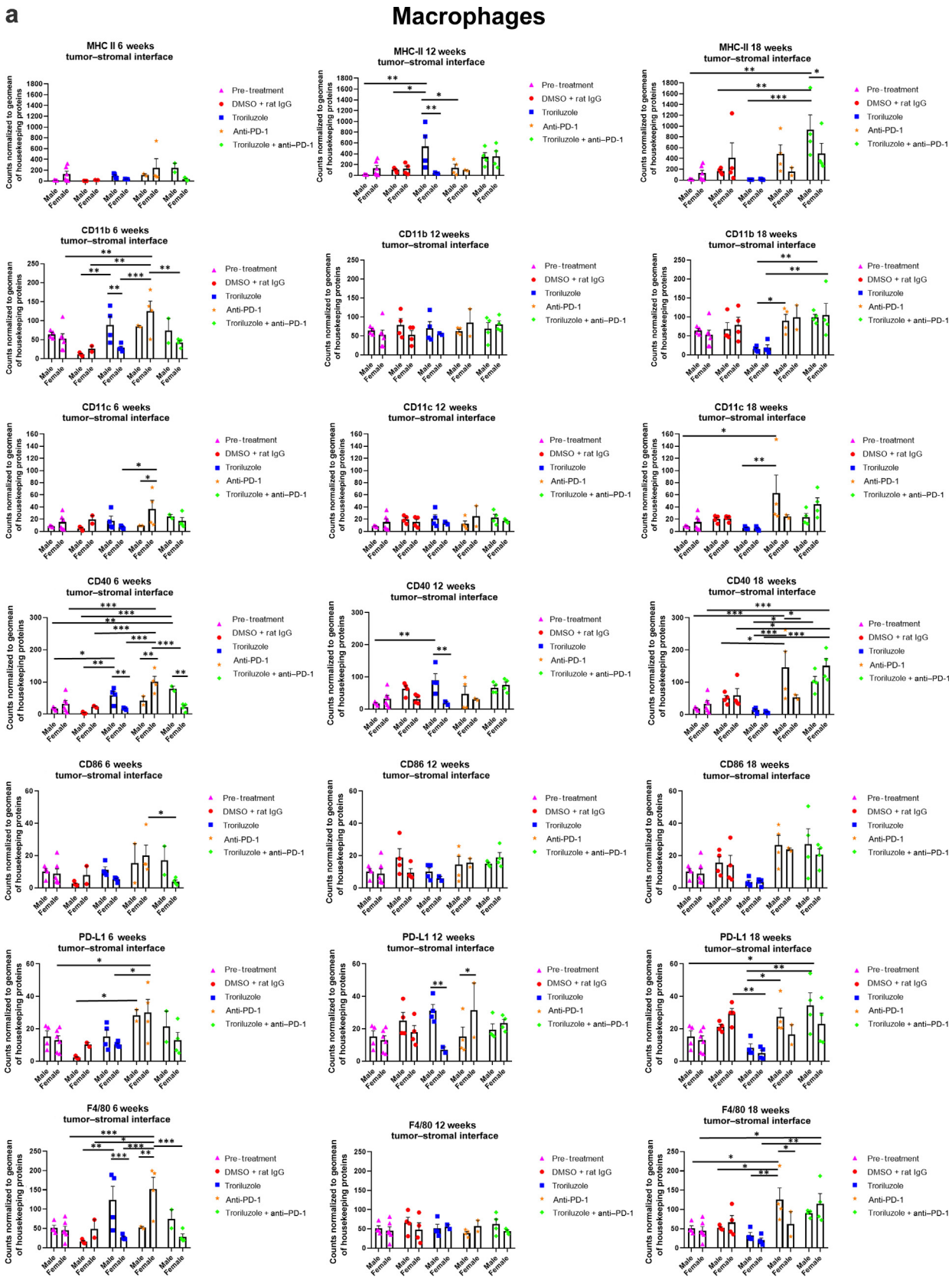

Figure 8. GeoMx digital spatial imaging profiles were performed to assess changes in the immune cell populations in the tumor–stromal interfaces over time. (**a**) Macrophages, (**b**) $CD8^+$ T cells, (**c**) cytotoxic T cells, (**d**) activated T cells, (**e**) $CD4^+$ T cells, (**f**) pan-immune cells. Values were average marker counts normalized to the geomean of the housekeeping gene ± SEM. The housekeeping proteins used for the normalization were histone H3 and S6 and were chosen because they correlated well with each other. The geomean of these markers was used for normalization because they take into consideration and control for outliers, whereas arithmetic mean does not. Pretreatment samples are skin specimens taken from male (n = 2) and female (n = 3) TGS mice aged 8 weeks that

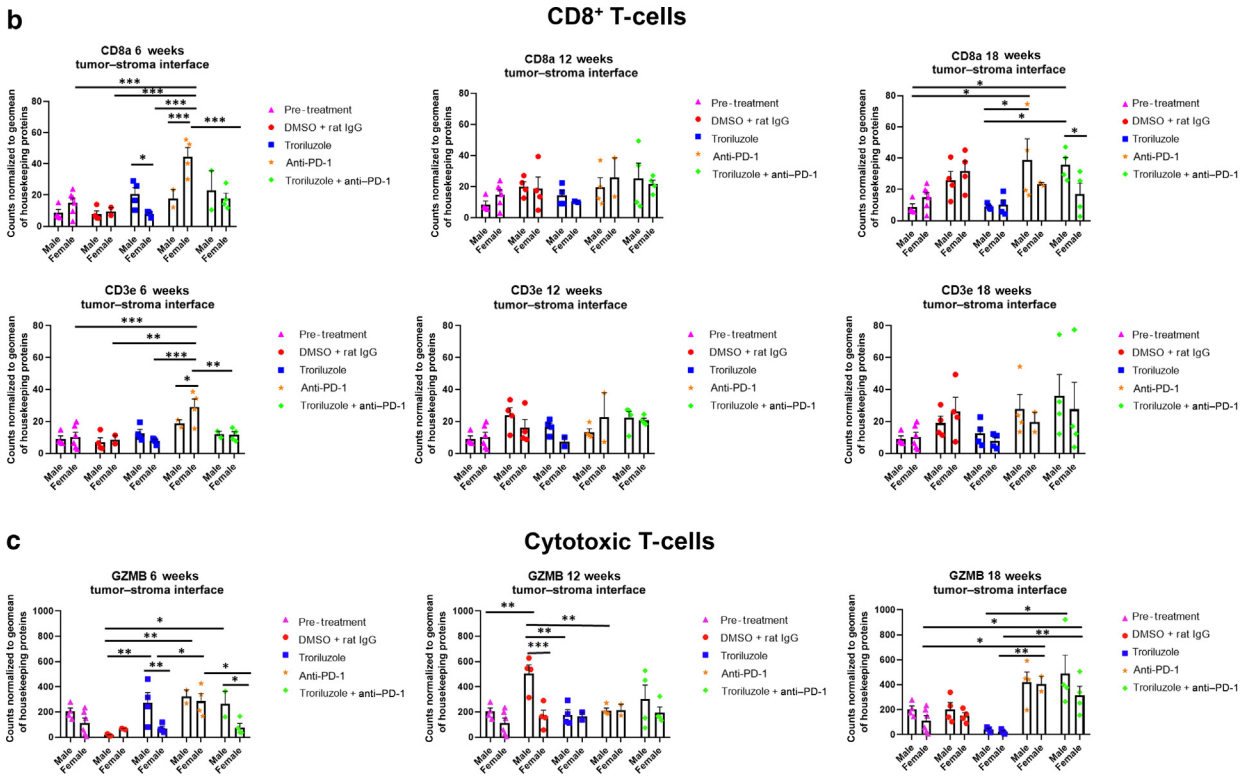

Figure 8. Continued.

the neoantigen load of tumors, therefore transforming a less antigenic tumor into a more antigenic tumor, which could increase the effectiveness of anti−PD-1 treatment.

This hypothesis was tested with the short-term therapeutic allograft and cell line−derived xenograft studies with troriluzole, a prodrug of riluzole, with or without anti−PD-1 (Eddy et al, 2023). Robust antitumor responses were observed after 25 days of treatment, with a reduction of 40−80% in short-term allograft or cell line−derived xenograft studies (Eddy et al, 2023). Extension of these short-term studies to a long-term study with a transgenic melanoma-prone mouse model with the exact treatment modalities yielded good antitumor efficacy as early as 6 weeks but gradually decreased with time (Eddy et al, 2023). When the dose of troriluzole was increased, no additional benefits were detected in male mice, whereas female mice now exhibited a much better response. Interestingly, the 2 treatment arms that yielded the best response in males were the troriluzole or anti−PD-1 monotherapy in both low and high doses of troriluzole.

It has been observed that in patients with cancer, sex differences occur in immune response while on immunotherapy regiments (Castro et al, 2020). Female patients with cancer have a more immunologically resistant tumor than male patients (Castro et al, 2020). Furthermore, the process of immune editing of a tumor is more robust in female patients than in male patients (Castro et al, 2020; Eddy and Chen, 2020; Escors, 2014; Ortona et al, 2019; Tucci et al, 2019). These results may contribute to the basis of why male patients respond to immunotherapy better than female patients (Ye

contain both dysplastic nevi (slightly raised pigmented lesions) and normal skin (no pigmented lesion) within the same skin specimen. The onset of melanoma in heterozygous TGS mice is 17−21 weeks, and prior to this, the nevi present are slightly raised ones—dysplastic nevi and flat pigmented lesions. As TGS mice aged, most of the slightly raised pigmented lesions became larger and thicker and are considered tumors. The pretreatment samples represent baseline levels of markers before treatment initiation, and the same values were used in the subsequent comparisons with 6-, 12-, and 18-week graphs. The threshold used to define change/no change for each marker and treatment arm took into consideration both the statistical analyses and the distribution of data points. At least 2 male and 2 female mice were used for each treatment arm except for 6 weeks (male, anti−PD-1 and troriluzole + anti−PD-1; female, DMSO + rat IgG), 12 weeks (female, troriluzole and anti−PD-1), and 18 weeks (female, anti−PD-1) where only 1 mouse was used. For each mouse specimen, at least 1−2 regions were selected. In the groups where only 1 mouse was used, 2 regions were selected from that sample. Regions of interest on the slides were selected by 3−4 individuals, with no specific criteria used to select regions from tumors and tumor−stromal interfaces. We had to include one of the individuals from the core facility at the University of Pittsburg Medical Center Cytometry Core because he had to label the samples each time. These specimens were made from tissue samples derived from mice randomly selected at each time point to be killed. Statistical analysis was conducted using a 2-way ANOVA test with Bonferroni posthoc comparisons to determine statistical significance between treated pairs at each time point, where the exposure variables were treatment groups and sex, and the outcome variable was marker values. To evaluate the statistical difference between 6 and 18 weeks for each marker and sex, a 2-way ANOVA was performed where the exposure variables were treatment groups and time points (6 and 18 weeks), and the outcome variable was marker value. $*P < .05$, $**P < .01$, and $***P < .001$. Markers used for immune profiling were chosen on the basis of whether the signal was above negative controls—Rb IgG, Rt IgG2a, and Rt IgG2b. The markers are as follows: MHC II, CD11b, CD11c, CD40, CD86, PD-L1, and F4/80 for macrophages; CD8a and CD3ε for $CD8^+$ T cells; GZMB for cytotoxic T cells; CD127/IL7RA, CD27, CD40L, CD44, and CTLA-4 for activated T cells; CD4, ICOS, and CD3ε for $CD4^+$ T cells; and CD45 for pan-immune cells. MHC II, major histocompatibility complex class II.

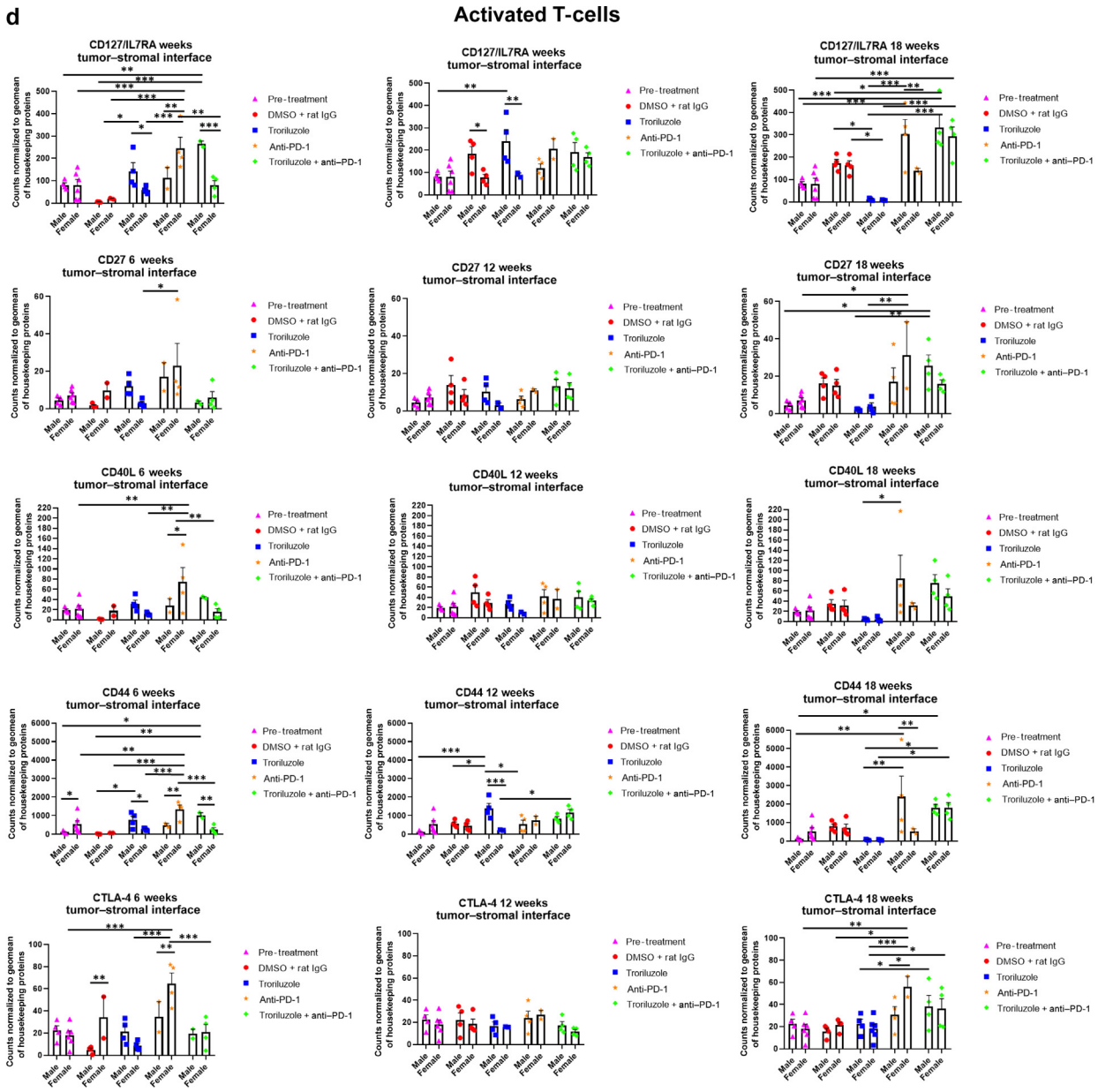

Figure 8. Continued.

et al, 2020). Ye et al (2020) have shown in a meta-analysis of clinical trial data for immune checkpoint blockade therapy that male patients with melanoma have better overall survival than female patients, which may correlate with tumor sequence variant burden, neoantigen load, PD-L1 expression, and density of anti-immune and proimmune cells (Ye et al, 2020). Furthermore, it is well-documented that females have lower incidences and mortality risk for melanoma than males, and recently, it has been suggested that this might be a result of sex hormone differences and/or immune system differences (Natale et al, 2018; Schwartz et al, 2019; White, 1959). Comparing the low-dose with high-dose troriluzole studies, we conclude that male mice benefited from both low and high doses of troriluzole, but at higher doses of troriluzole, male mice showed loss of responses at an earlier time point. In contrast, some female mice showed improved responses at the higher dose of troriluzole. It is possible that at a higher dose of troriluzole, there is increased bioavailability of the active drug, riluzole, in females, and this may be sufficient to transform a nonantigenic tumor into an antigenic one and overcome the tumors' intrinsic immune resistance, whereas in male mice, the higher dose of troriluzole may increase the selection process of male tumors to overcome the higher dose of troriluzole through tumor-intrinsic and/or tumor-extrinsic functions that led to a loss of response, and combining with anti−PD-1 was insufficient to overcome this blockade.

On the basis of the data from the GeoMx digital spatial imaging profiles, it is suggested that tumor-extrinsic functions in the tumor−stromal interfaces and tumors of male and female mice are likely responsible for the observed loss of response. Diminishing total immune cell populations,

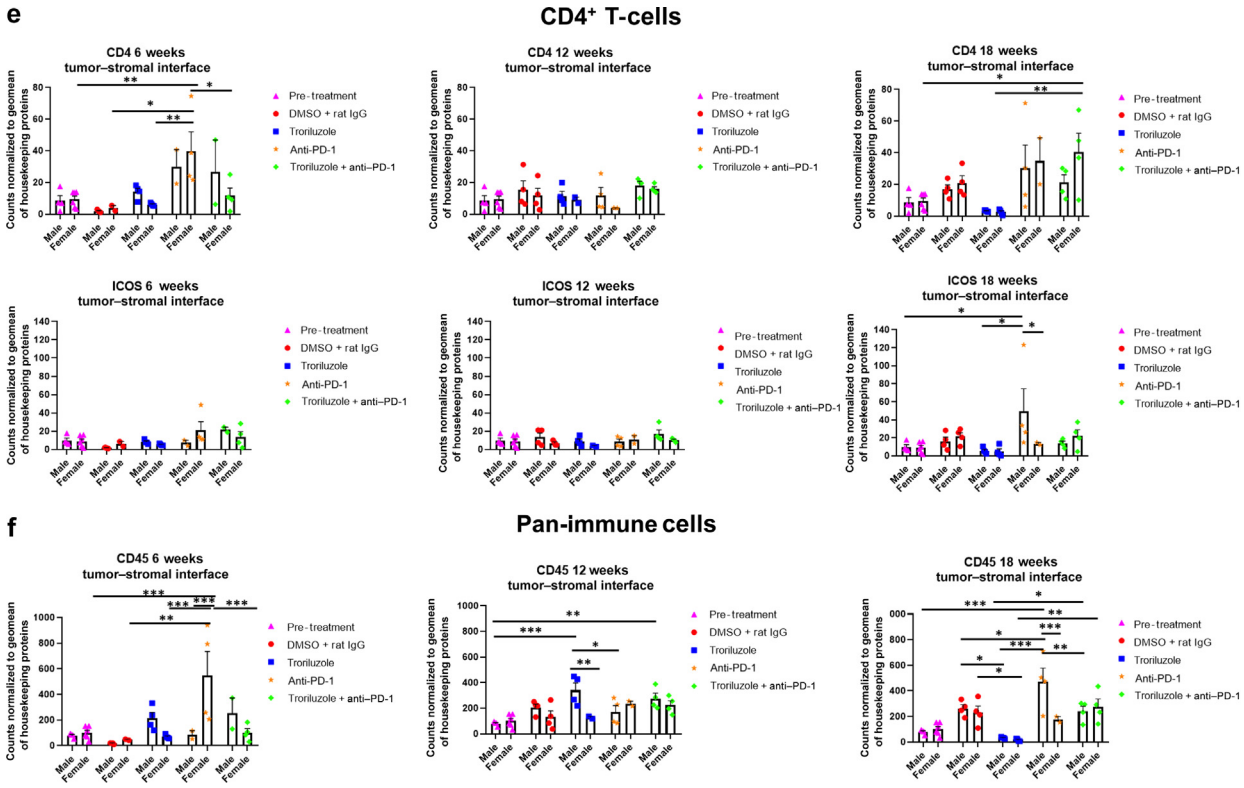

Figure 8. Continued.

including macrophages, CD4$^+$ T cells, and cytotoxic T cells, were noted, and a decrease in activated T cells in the tumor—stromal interfaces of male mice was observed. In tumors of male and female mice, there were no alterations in CD8$^+$ T cells (Figures 8 and 9). It is tempting to speculate that altering these immune cell populations in the tumors and tumor—stromal interfaces may lead to an increase in the antitumor immune response; however, further characterization of these immune cell populations and increasing the sample size are required to further test this hypothesis. To further delineate tumor-intrinsic functions that mediate a lack of response to troriluzole as a single agent and in combination with anti—PD-1, omic studies can be performed on TGS tumor samples from the lower- and higher-dose troriluzole study to investigate potential bypass mechanisms that might occur as a result of inhibiting glutamatergic signaling.

The contrasting results obtained from the short-term and long-term studies point to the importance of selecting the best available experimental model system to evaluate therapeutic response and performing studies using both male and female mice in evaluating the therapeutic index of compounds in animals (Barr et al, 2020; Li et al, 2019). Short-term graft studies are preclinical gold standards to validate molecular targets identified in omic screens and in vitro studies but are not necessarily sufficient to precisely evaluate the long-term therapeutic outcomes in patients. Furthermore, the maintenance of the tumor—stroma architecture is important for drug delivery and treatment response (Combest et al, 2012). It is tempting to speculate that the TGS mouse model and other similar ones may be useful to follow the development of loss of response to therapeutic regimens during drug development, and the knowledge acquired can be applied to patients in real time to improve patient survivability because this mouse model allows a 462 day (1.3 years) preclinical therapeutic study to be performed, whereas very few allograft/xenograft studies last >40 days.

MATERIALS AND METHODS

TGS mice

The immunocompetent hairless TGS mouse strain was developed by crosses between the immunocompetent strains of TG-3, a model that spontaneously develops metastatic melanoma, and SKH-1, an uncharacterized hairless mouse strain commonly used in dermatological studies (Benavides et al, 2009; Zhu et al, 2000, 1998). TGS mice allow for easy visualization and monitoring of tumor progression without the presence of fur (Eddy et al, 2023). Similar to TG-3, TGS mice also develop spontaneous melanoma with 100% penetrance (Eddy et al, 2023; Shah et al, 2019). All animal experiments were conducted in compliance with Rutgers University Institutional Animal Care and Use Committee guidelines (protocol number 999900047) and approved by Rutgers University Institutional Animal Care and Use Committee Committee.

Genotyping of TGS mice

TGS mice were genotyped to identify heterozygous mice from their wild-type and homozygous littermates, as previously described (Eddy et al, 2023).

Tumor progression in TGS mice

Tumor progression was monitored in TGS mice, as previously described, and was done in an independent and blinded fashion

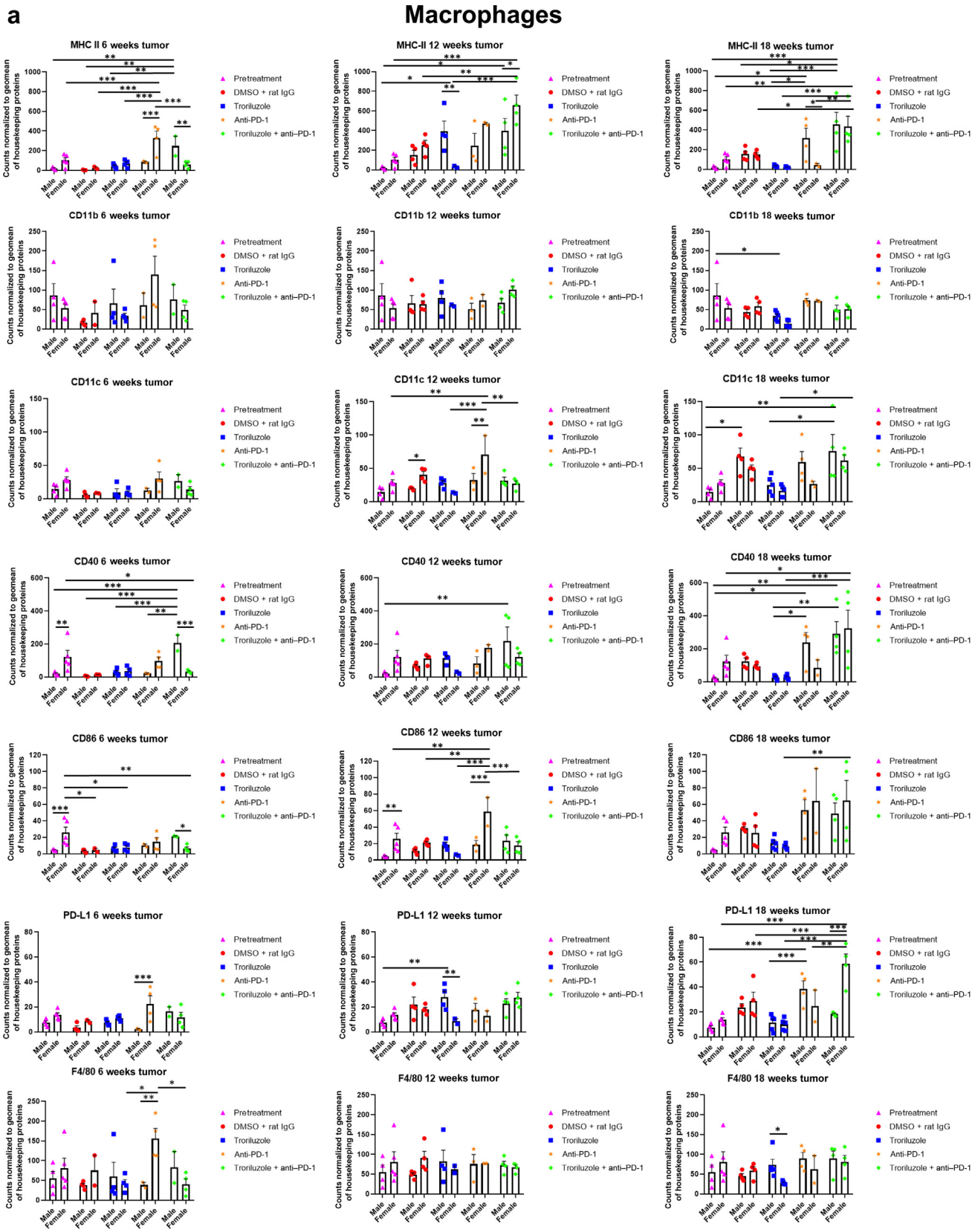

Figure 9. GeoMx digital spatial imaging profiles were performed to assess changes in the immune cell populations in the tumors over time. We followed the same process here as described in Figure 8, and the same slides were used as in Figure 8. Values were average marker counts normalized to geomean of housekeeping gene ± SEM. The housekeeping proteins used for the normalization were histone H3 and S6 and were chosen because they correlated well with each other. The geomean of these markers was used for normalization because they take into consideration and control for outliers, whereas arithmetic mean

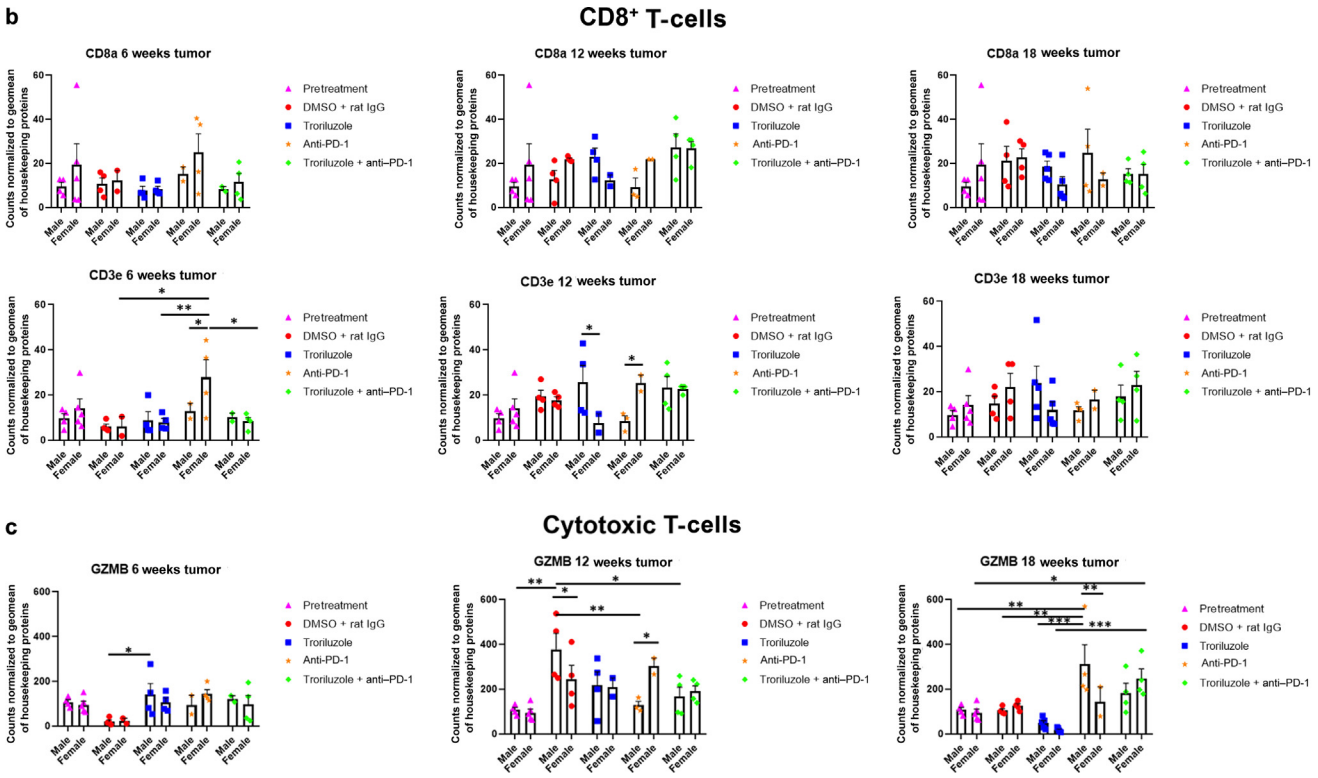

Figure 9. Continued.

(Eddy et al, 2023). IVIS, a small animal imaging system (IVIS Lumina LT series III, part number CLS136331, serial number 151312N6235, Perkin-Elmer, Hopkinton, MA) was used to monitor tumor progression with mice anesthetized with isoflurane, USP (NDC 46066-755-04, Pivetal Veterinary, Loveland, CO) through a nose cone within the IVIS machine. Images were captured by the IVIS system using visible light and permitted the mice to be placed at a preset distance between the camera and the mouse each time. Using a publicly available software program, ImageJ, developed by the National Institutes of Health (Bethesda, MD), lesions were quantified on the basis of the intensities of the lesions. Two 50 × 50-pixel area boxes were randomly positioned on the back of each mouse at the first acquisition of the image by IVIS. The same 2 boxes were used throughout the entire study to monitor tumor progression on the basis of previously saved images from each mouse. Each box was cropped, and the background was subtracted using a threshold of 4 pixels. The images were converted to binary and analyzed using the analyze particle feature. The 3-infinity size threshold (pixel^2) was used to define the minimum threshold; 2 and below were deemed to be background. The number and size of each pigmented lesion in each box were determined, and subsequent data analyses were performed using these values. Tumor burden was defined as the size and pigmentation of the tumors. No difference in tumor progression was noted over the course of the 18-week study in mice that started the study between 7 and 9 weeks (Table 2).

Treatments

Fox Chase Therapeutics Discovery (Doylestown, PA) provided lyophilized troriluzole (patent publication number US2021 0228549). Troriluzole hydrochloride (molecular weight: 419.09 g/mol) was dissolved in DMSO (catalog number D8418-1L, MilliporeSigma, Milwaukee, WI) to produce a stock solution of 100 mM, and a working solution was made with sterile PBS. Anti—PD-1 (clone RMP1-14, catalog number BE0146) and rat IgG (catalog number BE0089) were purchased from BioXCell (Lebanon, NH). Troriluzole and DMSO were administered 7 days per week by oral gavage; anti—PD-1 and rat IgG were administered 3 times during the first week and once per week thereafter by intraperitoneal injection.

Histopathology

Liver histopathology was performed as previously described (Eddy et al, 2023). Representative images from Figures 1b and 3c were taken from the HistoWiz website (https://home.histowiz.com/, Brooklyn, NY), and the liver H&E slides were further evaluated by HistoWiz pathologists.

Liquid chromatography—tandem mass spectrometry

Liquid chromatography—tandem mass spectrometry analyses were performed by Touchstone Biosciences (Plymouth Meeting, PA), as previously described (Eddy et al, 2023).

Protein lysate preparations from TGS mouse tumors

Tumor samples were flash frozen and stored at −80 °C until needed. Samples were added to a precooled mortar and pestle and were pulverized in liquid nitrogen. Once finely ground, the samples were added to a precooled 10 ml snap cap tube (catalog number 187262, Greiner Bio-one, Monroe, NC), and the appropriate volume of extraction buffer (lysis buffer, phosphatase inhibitor, and protease

does not. Markers used for immune profiling were chosen on the basis of whether the signal was above negative controls—Rb IgG, Rt IgG2a, and Rt IgG2b. The threshold used to define change/no change for each marker and treatment arm took into consideration both the statistical analyses and the distribution of data points. MHC II, major histocompatibility complex class II.

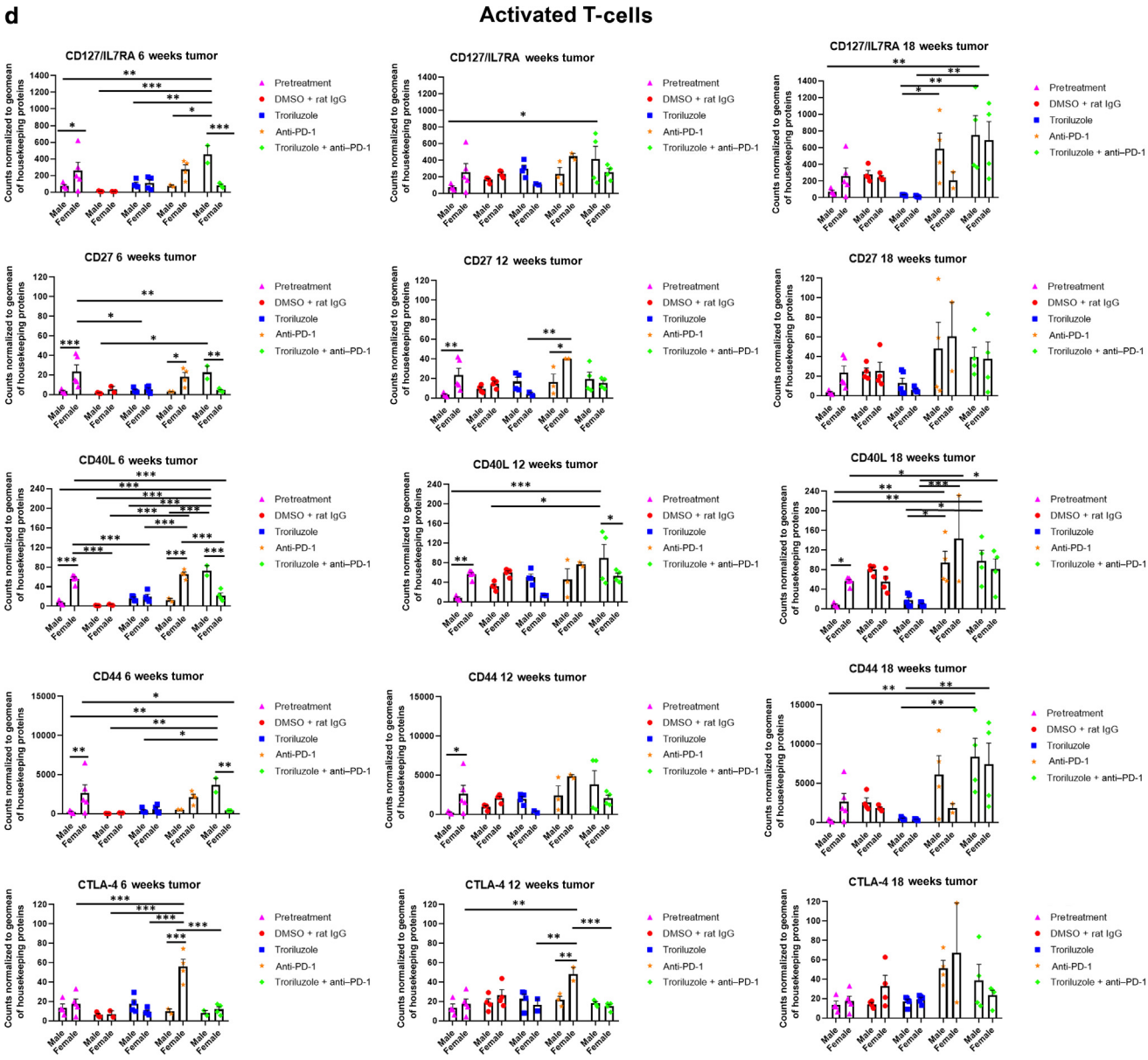

Figure 9. Continued.

inhibitor) was added depending on the sample size. The lysis buffer (pH 7.75) consisted of 50 mM Tris hydrochloride (catalog number T5941-1KG, MilliporeSigma), 150 mM sodium chloride (catalog number S9888-1KG, MilliporeSigma), 1 mM EDTA (catalog number EDS-100G, MilliporeSigma), 5% glycerol (catalog number G31-500, Thermo Fisher Scientific, Nazareth, PA), 1% Igepal (catalog number I3021-100mL, MilliporeSigma), and 1 mM DL-dithiothreitol (catalog number D9163-1G, MilliporeSigma). The composition of the 1 ml extraction buffer was 940 μl lysis buffer, 10 μl phosphatase inhibitor cocktail 2 (catalog number P5726-5mL, Sigma-Aldrich, St Louis, MO), 10 μl phosphatase inhibitor cocktail 3 (catalog number P0044-5mL, Sigma-Aldrich), and 40 μl protease inhibitor cocktail (catalog number 11836170001, MilliporeSigma). Samples were homogenized with the extraction buffer starting at 250 μl and incrementally increased to 1000 μl, with the volume used being dependent on the size of the sample tissue. A handheld homogenizer (catalog number TH115-PCR, OMNI International [a PerkinElmer company], Kennesaw, GA) was used in intervals of 10−15 seconds to avoid heat build up. Once homogenized, samples were rocked for 2 hours at 4 °C. Samples were centrifuged at 4 °C for 20 minutes at 18,407*g* to remove tissue debris, and the supernatant was stored at −80 °C until needed.

Western immunoblots

For the westerns, the following antibodies were used: mGluR1 (D5H10) (catalog number 12551S, Cell Signaling Technologies, Danvers, MA), GLS (catalog number NBP2-29940, Novus Biologicals, Littleton, CO), γ-H2AX (Ser 139) (clone JBW301, catalog number 05-636, Sigma-Aldrich), PD-L1 (catalog number 4059, ProSci Incorporated, Poway, CA), PD-1 clone 29F.1A12 (catalog number BE0273, BioXCell), tyrosinase (T311) (catalog number sc-20035, Santa Cruz Biotechnology, Dallas, TX), donkey anti-rabbit IgG horseradish peroxidase secondary antibody (catalog number AP182P, Sigma-Aldrich), goat anti-rat IgG horseradish peroxidase secondary antibody (catalog number AP136P, Sigma-Aldrich), and goat anti-mouse IgG horseradish peroxidase secondary antibody

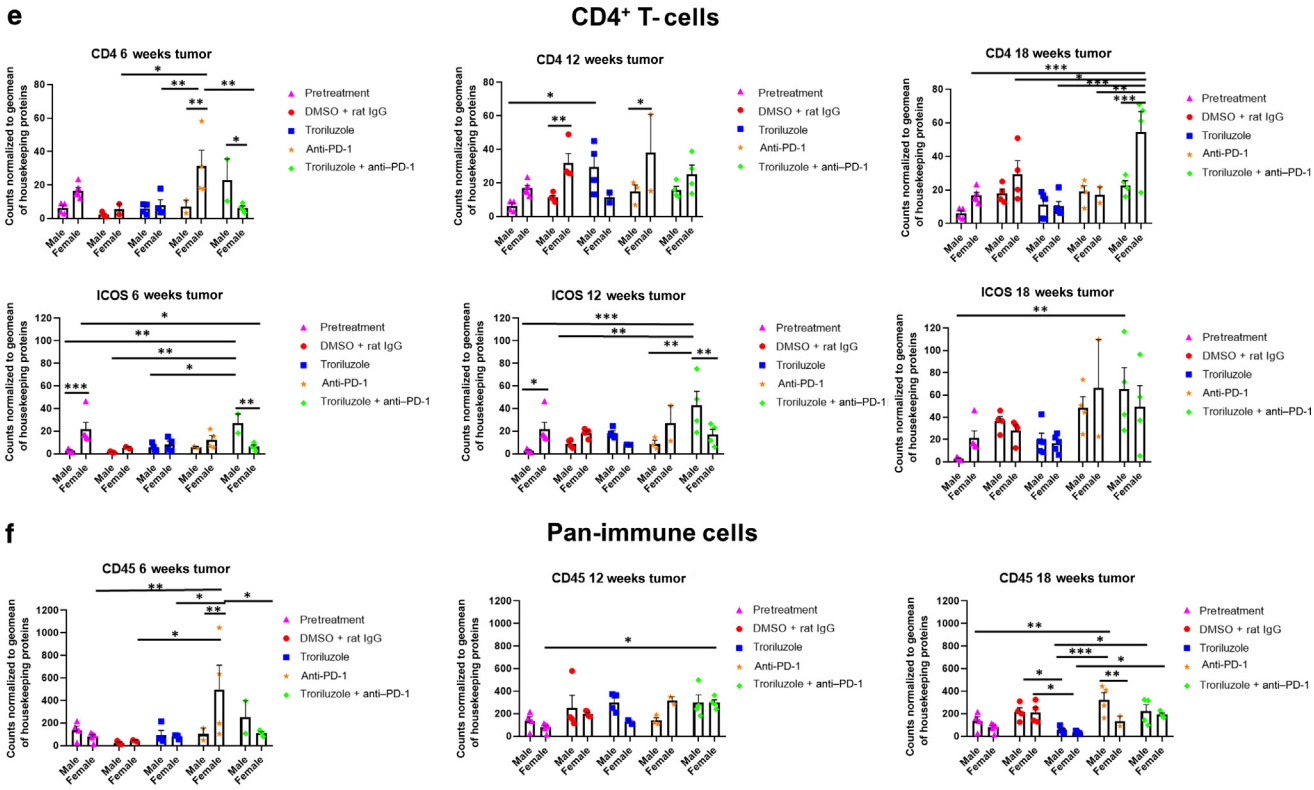

Figure 9. Continued.

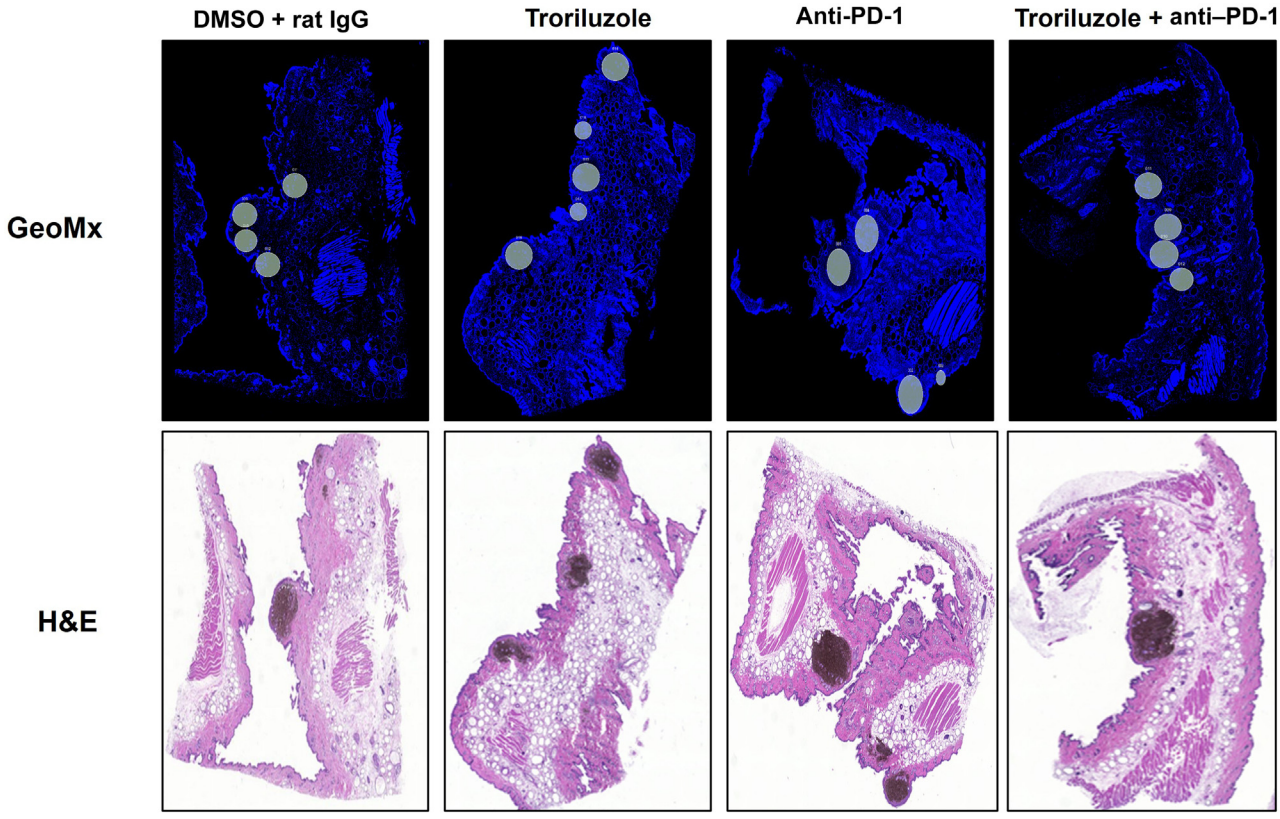

Figure 10. Representative images of data acquisition using the GeoMx digital spatial imaging platform. Regions on the GeoMx scans (above) were chosen on the basis of the location of the tumor–stromal interfaces and tumors on the H&E stains (bottom). Regions of interest on the slides were selected by 3–4 individuals; however, there were no specific criteria used to select tumors and tumor–stromal interfaces. We had to include 1 of the individuals from the core facility at the University of Pittsburg Medical Center Cytometry Core because he had to label the samples each time.

Table 2. Comparison of Tumor Progression Between TGS Mice Aged 7 and 9 Weeks

DMSO + Rat IgG

Mice	Sex	Age	Tumor Burden at 0 wk	Tumor Burden at 6 wk	Tumor Burden at 12 wk	Tumor Burden at 18 wk
2267	Male	7 wk 6 d	264	237	220	358
2268	Male	7 wk 6 d	157	227	310	426
2240	Male	8 wk 3 d	352	333	487	556
2241	Male	8 wk 3 d	382	471	533	703
2272	Male	9 wk	175	263	323	365
2273	Male	9 wk	189	338	364	387
2274	Male	9 wk	243	429	522	586
2275	Male	9 wk	334	401	544	624
2262	Female	7 wk 4 d	293	587	811	932
2263	Female	7 wk 4 d	436	242	312	302
2264	Female	7 wk 4 d	522	635	812	922
2265	Female	7 wk 4 d	410	496	561	633
2269	Female	7 wk 6 d	318	333	346	385
2270	Female	7 wk 6 d	177	307	418	459
2271	Female	7 wk 6 d	338	421	411	489
2282	Female	8 wk 4 d	338	472	504	519

Mice	Sex	Age	Fold Change at 0 wk	Fold Change at 6 wk	Fold Change at 12 wk	Fold Change at 18 wk
2267	Male	7 wk 6 d	1	0.897727273	0.833333333	1.356060606
2268	Male	7 wk 6 d	1	1.445859873	1.974522293	2.713375796
2240	Male	8 wk 3 d	1	0.946022727	1.383522727	1.579545455
2241	Male	8 wk 3 d	1	1.232984293	1.395287958	1.840314136
2272	Male	9 wk	1	1.502857143	1.845714286	2.085714286
2273	Male	9 wk	1	1.788359788	1.925925926	2.047619048
2274	Male	9 wk	1	1.765432099	2.148148148	2.411522634
2275	Male	9 wk	1	1.200598802	1.628742515	1.868263473
2262	Female	7 wk 4 d	1	2.003412969	2.767918089	3.180887372
2263	Female	7 wk 4 d	1	0.555045872	0.71559633	0.69266055
2264	Female	7 wk 4 d	1	1.216475096	1.555555556	1.766283525
2265	Female	7 wk 4 d	1	1.209756098	1.368292683	1.543902439
2269	Female	7 wk 6 d	1	1.047169811	1.088050314	1.210691824
2270	Female	7 wk 6 d	1	1.734463277	2.361581921	2.593220339
2271	Female	7 wk 6 d	1	1.24556213	1.215976331	1.446745562
2282	Female	8 wk 4 d	1	1.396449704	1.49112426	1.535502959

Troriluzole + anti–PD-1

Mice	Sex	Age	Tumor Burden at 0 wk	Tumor Burden at 6 wk	Tumor Burden at 12 wk	Tumor Burden at 18 wk
2373	Male	8 wk 5 d	192	199	271	353
2374	Male	8 wk 5 d	172	361	571	652
2433	Male	7 wk 5 d	243	335	462	543
2434	Male	7 wk 5 d	424	321	303	406
2435	Male	7 wk 5 d	341	215	149	260
2436	Male	7 wk 5 d	107	123	216	262
2438	Male	7 wk 3 d	153	336	519	539
2448	Male	7 wk 3 d	206	185	335	479

Mice	Sex	Age	Fold Change at 0 wk	Fold Change at 6 wk	Fold Change at 12 wk	Fold Change at 18 wk
2373	Male	8 wk 5 d	1	1.036458333	1.411458333	1.838541667
2374	Male	8 wk 5 d	1	2.098837209	3.319767442	3.790697674
2433	Male	7 wk 5 d	1	1.378600823	1.901234568	2.234567901
2434	Male	7 wk 5 d	1	0.757075472	0.714622642	0.95754717
2435	Male	7 wk 5 d	1	0.630498534	0.436950147	0.762463343
2436	Male	7 wk 5 d	1	1.14953271	2.018691589	2.448598131
2438	Male	7 wk 3 d	1	2.196078431	3.392156863	3.522875817
2448	Male	7 wk 3 d	1	0.898058252	1.626213592	2.325242718

Top, DMSO + rat IgG; bottom, troriluzole + anti–PD-1. Tumor burden (units: pixel^2) was defined as the size and pigmentation of the tumors.

(catalog number A4416-1ML, Sigma-Aldrich). The following procedures were followed. Tumor extracts were prepared for western immunoblots as follows: 5× sample dye (250 mM Tris hydrochloride [catalog number T5941-1KG, MilliporeSigma], 10% SDS [catalog number 811030-1KG, VWR-MP Biomedicals, Solon, OH], and 0.05% bromophenol blue [catalog number B0126-25G, MilliporeSigma]) was diluted to 1× with 2-mercaptoethanol (catalog number M6250-500mL, MilliporeSigma) and 85% glycerol (catalog number G31-500, Thermo Fisher Scientific)]. For every 5 µl of total volume loaded onto the western, there was 1 µl of 1× sample dye, and a volume of lysis buffer (buffer used in the original extraction) was used to bring the solution to the final volume. Samples were denatured on a glycerol heat block for 5 minutes at 95 °C, except for mGluR1, which was denatured at 65 °C and immediately placed on ice before loading.

Samples were loaded onto a 10% SDS-PAGE and electrophoresed for 2−3 hours at 120 volts depending on the protein of interest. A reference prestained protein ladder (catalog number 26619, Thermo Fisher Scientific, Waltham, MA) (10 µl) was loaded alongside the samples to determine the molecular weights of proteins. Proteins on the gel were transferred onto a nitrocellulose membrane (catalog number 10600002, MilliporeSigma) at 4 °C for 3 hours at 160 mAmps. The membrane was stained with Ponceau S solution (catalog number P7170-1L, MilliporeSigma) to validate that the proteins were successfully transferred. The membrane was then cut on the basis of the molecular weight of the protein of interest and blocked for 1 hour in 5% milk at room temperature. The membrane was placed in a bag with a 0.25% milk solution with the corresponding primary antibody and was left rocking at 4 °C overnight. The next day, the membrane was washed twice for 5 minutes each and incubated in the respective secondary antibodies for 1 hour at room temperature. After incubation, the membrane was washed 6 times for 5 minutes each time. Immobilon crescendo western horseradish peroxidase substrate (catalog number WBLUR0100, Sigma-Aldrich) was added onto the membrane and incubated for 3 minutes in darkness. Membranes were imaged using the imaging machine, GeneGnome XRQ GENESys, and the accompanying computer program (serial number SYGN0/04028, Syngene A Division of the Synoptics Group, New City, NY, program V1.5.0.0). ImageJ, the computer software developed by the National Institute of Health, was used to quantify the band intensities.

For the westerns that used the antibodies, xCT (catalog number ANT-111, Alomone, Jerusalem, Israel), EAAT2 (catalog number A3679, Abclonal, Woburn, MA), tyrosinase (catalog number sc-20035, Santa Cruz Biotechnology), IRDye 680RD goat anti-rabbit IgG secondary antibody (catalog number 926-68071, LI-COR, Lincoln, NE), or IRDye 800CW goat anti-mouse IgG secondary antibody (catalog number 926-32210, LI-COR) were used. The following procedures were used. Tissue lysates containing a final concentration of 1X LDS sample buffer (catalog number NP0007, Invitrogen, Carlsbad, CA) and 2.5% 2-Mercaptoethanol (catalog number 60-24-2, Sigma-Aldrich) were loaded onto a 12% Bis-Tris gel (catalog number NW00125BOX, Invitrogen). After gel electrophoresis, proteins were transferred to a membrane using iBlot 2 Gel Transfer Device (catalog number IB21001, Invitrogen, Kiryat Shmona, Israel). Membranes were blocked for 1 hour at room temperature in blocking buffer (catalog number 927-60001, LI-COR), and primary antibodies were diluted in antibody diluent (catalog number 927-65001, LI-COR) overnight at 4 °C except for tyrosinase. The following day, blots were washed for 5 minutes 4 times. Membranes with tyrosinase (catalog number sc-20035, Santa Cruz Biotechnology) were diluted in antibody diluent (catalog number 927-65001, LI-COR) and incubated for 1 hour at room temperature. After primary antibody incubations, blots were washed for 5 minutes 4 times. Secondary antibodies were diluted in antibody diluent (catalog number 27-65001, LI-COR) containing 0.1% SDS (catalog number 46-040-CL, Corning, Manassas, VA) for 45 minutes at room temperature. Blots were washed for 5 minutes 4 times. Blots were imaged using the LI-COR Odyssey imaging system (Odyssey CLx, serial number CLX-2442, LI-COR) and normalized using LI-COR Empiria Studio software (Biosciences V2.1.0.134, LI-COR).

NanoString GeoMx digital spatial imaging profiling

Formalin fixation and paraffin embedding of tumors were performed as follows. Tumors were harvested from all treatment arms during necropsy after 18 weeks of treatment and immediately placed into 10% neutral buffered formalin (catalog number HT501128-4L, Sigma-Aldrich, Allentown, PA). After 72 hours, formalin was replaced with 70% ethanol (catalog number ES753, Azer Scientific, Morgantown, PA). The samples were stored until they were processed to paraffin blocks using the LEICA TP1020 (serial number 8364, Leica Biosystems, Vista, CA) for tissue processing, and for tissue embedding, the Tissue-Tek TEC 5 embedding and cryo module (model number TEC 5 EM A-1, Sakura Finetek USA [for embedding module] and model number TEC 5 CM A-1 [for cryo module] was used. Formalin-fixed and paraffin-embedded blocks were sectioned using a Microm HM 315 Microtome (GmbH SKU# 8243-30-1007, MICROM International, Walldorf, Germany). Slides (catalog number 12-550-15, Thermo Fisher Scientific) were shipped to the University of Pittsburg Medical Center Cytometry Core for staining of the slides and data acquisition. The immune cell profiling and the immune activation status panels were used. Each panel was a mixture of antibody cocktails that were sold by NanoString. Once data were acquired, quality control and data normalization were performed using the GeoMx DSP analysis suite following the guidelines provided by NanoString. The readouts of the data were in counts and normalized to counts of geomean of housekeeping proteins. The housekeeping proteins used for the normalization were histone H3 and S6 and were chosen because they correlated well with each other. The geomean of these markers was used for normalization because they take into consideration and control for outliers, whereas arithmetic mean does not. Markers used for immune profiling were chosen on the basis of whether the signal was above negative controls: Rb IgG, Rt IgG2a, and Rt IgG2b. The data that had undergone quality control and normalization were downloaded as Excel files from the analysis suite, and subsequent data analyses were performed using GraphPad Prism for graphical representation of the data and StatPlus Pro software from AnalystSoft plug-in in Microsoft Excel for statistical analysis.

Statistical analysis

Appropriate sample sizes for animal studies were determined in consultation with the University Biometrics Facility Core. Statistical significance was determined using StatPlus Pro software from the AnalystSoft plug-in in Microsoft Excel. Analyses were conducted using either a 1-way or 2-way ANOVA test depending on the variable(s) being tested, and Bonferroni posthoc analyses were performed to determine statistical significance between treated pairs, and the threshold for significance can be found in each figure or

table legend as well as the exposure and outcome variables. GraphPad Prism was used to create the Kaplan–Meier survival curves and to perform Log-rank (Mantel–Cox) and Gehan–Breslow–Wilcoxon statistical tests to determine statistical significance between survival curves.

ETHICS STATEMENT

All animal experiments were conducted in compliance with Rutgers Institutional Animal Care and Use Committee guidelines (protocol number 999900047) and approved by Rutgers Institutional Animal Care and Use Committee Committee.

DATA AVAILABILITY STATEMENT

All materials, data, and protocols will be provided upon request. Minimal datasets necessary to interpret and/or replicate data in this paper are available upon request to the corresponding author. No large datasets were generated or analyzed during this study.

ORCIDs

Kevinn Eddy: http://orcid.org/0000-0003-3531-6331
Kajal Gupta: http://orcid.org/0000-0002-0665-1539
Mohamad Naser Eddin: http://orcid.org/0000-0001-8982-6025
Christina Marinaro: http://orcid.org/0000-0002-1979-0167
Sanjana Putta: http://orcid.org/0000-0002-5141-6474
John Michael Sauer Jr: http://orcid.org/0009-0009-5083-2028
Anna Chaly: http://orcid.org/0000-0002-6726-7063
Katie B. Freeman: http://orcid.org/0000-0003-4021-8808
Jeffrey C. Pelletier: http://orcid.org/0000-0002-0397-0681
Anna Fateeva: http://orcid.org/0000-0003-1801-434X
Philip Furmanski: http://orcid.org/0009-0003-3931-3004
Ann W. Silk: http://orcid.org/0000-0003-3877-3984
Allen B. Reitz: http://orcid.org/0000-0003-2780-4044
Andrew Zloza: http://orcid.org/0000-0001-8844-6493
Suzie Chen: http://orcid.org/0000-0002-6384-5081

CONFLICT OF INTEREST

JCP and ABR have an equity interest in Biohaven Pharmaceuticals. AWS reports on research funding to her institution from Biohaven Pharmaceuticals, which is the manufacturer of one of the agents used in the experiments (troriluzole). Employees at Fox Chase Therapeutics Discovery report interest in troriluzole, which was discovered at Fox Chase Therapeutics Discovery, followed by an Agreement with Biohaven Pharmaceuticals, which is developing it commercially.

ACKNOWLEDGMENTS

This research was supported by the National Cancer Institute Small Business Innovation Research (R44CA156781-04) to ABR and SC and the Veterans Administration Research Merit Award (101BX003742) to SC. SC and KE are grateful for the support from the New Jersey Commission on Cancer Research Pre-Doctoral Fellowship (DCHS19PPC027) and the Rutgers University and Louis Bevier Completion Fellowship. SC, KE, and AF are grateful for the Rutgers Molecular Biosciences Excellence Fellowship. Troriluzole is an experimental small-molecule therapeutic agent from Biohaven Pharmaceuticals currently under phase II/III clinical studies for neurological and oncology indications. We appreciate the insightful comments provided throughout this study by Darren Carpizo, Shridar Ganesan, and Kathleen Scotto that have helped shape this project. We would like to thank the Rutgers Veterinary staff for the care and maintenance of our mice. We are grateful to Ernest Meyer at the University of Pittsburg Medical Center Cytometry Core for performing the GeoMx Digital Spatial Imaging Profiling assays and for his invaluable advice throughout the process as well as Clement David at NanoString for his advice during the quality control and data analysis steps of the assays. This work is in partial fulfillment of the requirements for the degree of Doctor of Philosophy from the Rutgers University School of Graduate Studies for KE.

AUTHOR CONTRIBUTIONS

Conceptualization: KE, JCP, AWS, ABR, AZ, SC; Data Curation: KE, ABR, AZ, SC; Formal Analysis: KE, KG, ABR, AZ, SC; Funding Acquisition: KE, AWS, ABR, AZ, SC; Investigation: KE, KG, MNE, CM, SP, JMS, AC, KBF, SC; Methodology: KE, KG, JCP, PF, ABR, AZ, SC; Project Administration: KE, SC; Resources: KE, KG, JCP, ABR, AZ, SC; Supervision: KE, KG, ABR, AZ, SC; Validation: KE, KG, JCP, ABR, AZ, SC; Visualization: KE, AF, PF, SC; Writing – Original Draft Preparation: KE, SC; Writing – Review and Editing: KE, KG, MNE, CM, SP, JMS, AC, KBF, JCP, AF, PF, AWS, ABR, AZ, SC

Disclaimer

The funders and Biohaven Pharmaceuticals were not involved in the study design; collection, analysis, interpretation of data; the writing of this article; or the decision to submit it for publication.

REFERENCES

Alb M, Sie C, Adam C, Chen S, Becker JC, Schrama D. Cellular and cytokine-dependent immunosuppressive mechanisms of grm1-transgenic murine melanoma. Cancer Immunol Immunother 2012;61:2239–49.

Barr JT, Tran TB, Rock BM, Wahlstrom JL, Dahal UP. Strain-dependent variability of early discovery small molecule pharmacokinetics in mice: does strain matter? Drug Metab Dispos 2020;48:613–21.

Benavides F, Oberyszyn TM, VanBuskirk AM, Reeve VE, Kusewitt DF. The hairless mouse in skin research. J Dermatol Sci 2009;53:10–8.

Carbone M, Duty S, Rattray M. Riluzole elevates GLT-1 activity and levels in striatal astrocytes. Neurochem Int 2012;60:31–8.

Castro A, Pyke RM, Zhang X, Thompson WK, Day CP, Alexandrov LB, et al. Strength of immune selection in tumors varies with sex and age. Nat Commun 2020;11:4128.

Cerchio R Jr, Marinaro C, Foo TK, Xia B, Chen S. Nonhomologous end-joining repair is likely involved in the repair of double-stranded DNA breaks induced by riluzole in melanoma cells. Melanoma Res 2020;30:303–8.

Chen HC, Sierra J, Yu LJ, Cerchio R Jr, Wall BA, Goydos J, et al. Activation of Grm1 expression by mutated BRaf (V600E) in vitro and in vivo. Oncotarget 2018;9:5861–75.

Chen S, Zhu H, Wetzel WJ, Philbert MA. Spontaneous melanocytosis in transgenic mice. J Invest Dermatol 1996;106:1145–51.

Clark CA, Gupta HB, Sareddy G, Pandeswara S, Lao S, Yuan B, et al. Tumor-intrinsic PD-L1 signals regulate cell growth, pathogenesis, and autophagy in ovarian cancer and melanoma [published correction for Cancer Res 2017;77:2770. Cancer Res 2016;76:6964–74.

Combest AJ, Roberts PJ, Dillon PM, Sandison K, Hanna SK, Ross C, et al. Genetically engineered cancer models, but not xenografts, faithfully predict anticancer drug exposure in melanoma tumors. Oncologist 2012;17:1303–16.

Eddy K, Chen S. Overcoming immune evasion in melanoma. Int J Mol Sci 2020;21:8984.

Eddy K, Chen S. Glutamatergic signaling a therapeutic vulnerability in melanoma. Cancers (Basel) 2021;13:3874.

Eddy K, Eddin MN, Fateeva A, Pompili SVB, Shah R, Doshi S, et al. Implications of a neuronal receptor family, metabotropic glutamate receptors, in cancer development and progression. Cells 2022;11:2857.

Eddy K, Gupta K, Pelletier JC, Isola AL, Marinaro C, Rasheed MA, et al. A spontaneous melanoma mouse model applicable for a longitudinal chemotherapy and immunotherapy study. J Invest Dermatol 2023;143:2007–18.e6.

Eisenhauer EA, Therasse P, Bogaerts J, Schwartz LH, Sargent D, Ford R, et al. New response evaluation criteria in solid tumours: revised RECIST guideline (version 1.1). Eur J Cancer 2009;45:228–47.

Escors D. Tumour immunogenicity, antigen presentation and immunological barriers in cancer immunotherapy. New J Sci 2014;2014:734515.

Fang T, Al Khleifat A, Meurgey JH, Jones A, Leigh PN, Bensimon G, et al. Stage at which riluzole treatment prolongs survival in patients with amyotrophic lateral sclerosis: a retrospective analysis of data from a dose-ranging study. Lancet Neurol 2018;17:416–22.

Hernandez S, Lazcano R, Serrano A, Powell S, Kostousov L, Mehta J, et al. Challenges and opportunities for immunoprofiling using a spatial high-plex technology: the NanoString GeoMx digital spatial profiler. Front Oncol 2022;12:890410.

Kleffel S, Posch C, Barthel SR, Mueller H, Schlapbach C, Guenova E, et al. Melanoma cell-intrinsic PD-1 receptor functions promote tumor growth. Cell 2015;162:1242–56.

Li F, Ulrich ML, Shih VF, Cochran JH, Hunter JH, Westendorf L, et al. Mouse strains influence clearance and efficacy of antibody and antibody-drug conjugate via Fc-FcγR interaction. Mol Cancer Ther 2019;18:780–7.

Mairhofer DG, Ortner D, Tripp CH, Schaffenrath S, Fleming V, Heger L, et al. Impaired gp100-specific CD8(+) T-cell responses in the presence of myeloid-derived suppressor cells in a spontaneous mouse melanoma model. J Invest Dermatol 2015;135:2785–93.

Marín YE, Namkoong J, Cohen-Solal K, Shin SS, Martino JJ, Oka M, et al. Stimulation of oncogenic metabotropic glutamate receptor 1 in melanoma cells activates ERK1/2 via PKCepsilon. Cell Signal 2006;18:1279–86.

Medikonda R, Choi J, Pant A, Saleh L, Routkevitch D, Tong L, et al. Synergy between glutamate modulation and anti-programmed cell death protein 1 immunotherapy for glioblastoma. J Neurosurg 2021;136:379–88.

Mehnert JM, Silk AW, Lee JH, Dudek L, Jeong BS, Li J, et al. A phase II trial of riluzole, an antagonist of metabotropic glutamate receptor 1 (GRM1) signaling, in patients with advanced melanoma. Pigment Cell Melanoma Res 2018;31:534–40.

Namkoong J, Shin SS, Lee HJ, Marín YE, Wall BA, Goydos JS, et al. Metabotropic glutamate receptor 1 and glutamate signaling in human melanoma. Cancer Res 2007;67:2298–305.

Natale CA, Li J, Zhang J, Dahal A, Dentchev T, Stanger BZ, et al. Activation of G protein-coupled estrogen receptor signaling inhibits melanoma and improves response to immune checkpoint blockade. ELife 2018;7:e31770.

Ohtani Y, Harada T, Funasaka Y, Nakao K, Takahara C, Abdel-Daim M, et al. Metabotropic glutamate receptor subtype-1 is essential for in vivo growth of melanoma. Oncogene 2008;27:7162–70.

Ortona E, Pierdominici M, Rider V. Editorial: sex hormones and gender differences in immune responses. Front Immunol 2019;10:1076.

Pollock PM, Cohen-Solal K, Sood R, Namkoong J, Martino JJ, Koganti A, et al. Melanoma mouse model implicates metabotropic glutamate signaling in melanocytic neoplasia. Nat Genet 2003;34:108–12.

Prokopi A, Tripp CH, Tummers B, Hornsteiner F, Spoeck S, Crawford JC, et al. Skin dendritic cells in melanoma are key for successful checkpoint blockade therapy. J Immunother Cancer 2021;9:e000832.

Schwartz MR, Luo L, Berwick M. Sex differences in melanoma. Curr Epidemiol Rep 2019;6:112–8.

Shah R, Chen S. Metabolic signaling cascades prompted by glutaminolysis in cancer. Cancers (Basel) 2020;12:2624.

Shah R, Singh SJ, Eddy K, Filipp FV, Chen S. Concurrent targeting of glutaminolysis and metabotropic glutamate receptor 1 (GRM1) reduces glutamate bioavailability in GRM1+ melanoma. Cancer Res 2019;79:1799–809.

Shin SS, Jeong BS, Wall BA, Li J, Shan NL, Wen Y, et al. Participation of xCT in melanoma cell proliferation in vitro and tumorigenesis in vivo. Oncogenesis 2018;7:86.

Shin SS, Namkoong J, Wall BA, Gleason R, Lee HJ, Chen S. Oncogenic activities of metabotropic glutamate receptor 1 (Grm1) in melanocyte transformation. Pigment Cell Melanoma Res 2008;21:368–78.

Shin SS, Wall BA, Goydos JS, Chen S. AKT2 is a downstream target of metabotropic glutamate receptor 1 (Grm1). Pigment Cell Melanoma Res 2010;23:103–11.

Siegel RL, Giaquinto AN, Jemal A. Cancer statistics, 2024. CA Cancer J Clin 2024;74:12–49.

Silk AW, Saraiya B, Groisberg R, Chan N, Spencer K, Girda E, et al. A phase Ib dose-escalation study of troriluzole (BHV-4157), an oral glutamatergic signaling modulator, in combination with nivolumab in patients with advanced solid tumors. Eur J Med Res 2022;27:107.

Somasundaram R, Connelly T, Choi R, Choi H, Samarkina A, Li L, et al. Tumor-infiltrating mast cells are associated with resistance to anti-PD-1 therapy. Nat Commun 2021;12:346.

Tucci M, Passarelli A, Mannavola F, Felici C, Stucci LS, Cives M, et al. Immune system evasion as hallmark of melanoma progression: the role of dendritic cells. Front Oncol 2019;9:1148.

van Kan HJ, Groeneveld GJ, Kalmijn S, Spieksma M, van den Berg LH, Guchelaar HJ. Association between CYP1A2 activity and riluzole clearance in patients with amyotrophic lateral sclerosis. Br J Clin Pharmacol 2005;59:310–3.

Wall BA, Wangari-Talbot J, Shin SS, Schiff D, Sierra J, Yu LJ, et al. Disruption of GRM1-mediated signalling using riluzole results in DNA damage in melanoma cells. Pigment Cell Melanoma Res 2014;27:263–74.

Wang Q, Xie B, Liu S, Shi Y, Tao Y, Xiao D, et al. What happens to the immune microenvironment after PD-1 inhibitor therapy? Front Immunol 2021;12:773168.

Wang X, Yang X, Zhang C, Wang Y, Cheng T, Duan L, et al. Tumor cell-intrinsic PD-1 receptor is a tumor suppressor and mediates resistance to PD-1 blockade therapy. Proc Natl Acad Sci USA 2020;117:6640–50.

Wangari-Talbot J, Wall BA, Goydos JS, Chen S. Functional effects of GRM1 suppression in human melanoma cells. Mol Cancer Res 2012;10:1440–50.

White LP. Studies on melanoma. II. Sex and survival in human melanoma. N Engl J Med 1959;260:789–97.

Ye Y, Jing Y, Li L, Mills GB, Diao L, Liu H, et al. Sex-associated molecular differences for cancer immunotherapy. Nat Commun 2020;11:1779.

Yip D, Le MN, Chan JL, Lee JH, Mehnert JA, Yudd A, et al. A phase 0 trial of riluzole in patients with resectable stage III and IV melanoma. Clin Cancer Res 2009;15:3896–902.

Zhu H, Reuhl K, Botha R, Ryan K, Wei J, Chen S. Development of early melanocytic lesions in transgenic mice predisposed to melanoma. Pigment Cell Res 2000;13:158–64.

Zhu H, Reuhl K, Zhang X, Botha R, Ryan K, Wei J, et al. Development of heritable melanoma in transgenic mice. J Invest Dermatol 1998;110:247–52.

Zhu H, Ryan K, Chen S. Cloning of novel splice variants of mouse mGluR1. Brain Res Mol Brain Res 1999;73:93–103.